JUSTUS-LIEBIG-UNIVERSITÄT GIESSEN

DOCTORAL THESIS

Development and Characterization of a Cold Atmospheric Plasma Source for Clinical Application

Entwicklung und Charakterisierung einer kalten atmosphärischen Plasmaquelle zur klinischen Anwendung

---

Author:
Sandra MORITZ

Supervisor:
Prof. Dr. Markus H. THOMA

A cumulative thesis submitted in fulfillment of the requirements for the degree of Dr. rer. nat.

in the

AG Atom-, Plasma- und Raumfahrtphysik
I. Physikalisches Institut

June 13, 2025

Declaration of Authorship

Ich erkläre: Ich habe die vorgelegte Dissertation selbstständig und ohne unerlaubte fremde Hilfe und nur mit den Hilfen angefertigt, die ich in der Dissertation angegeben habe. Alle Textstellen, die wörtlich oder sinngemäß aus veröffentlichten Schriften entnommen sind, und alle Angaben, die auf mündlichen Auskünften beruhen, sind als solche kenntlich gemacht. Ich stimme einer evtl. Überprüfung meiner Dissertation durch eine Antiplagiat-Software zu. Bei den von mir durchgeführten und in der Dissertation erwähnten Untersuchungen habe ich die Grundsätze guter wissenschaftlicher Praxis, wie sie in der „Satzung der Justus-Liebig-Universität Gießen zur Sicherung guter wissenschaftlicher Praxis“ niedergelegt sind, eingehalten.

Angaben zu auf künstlicher Intelligenz (KI) basierender Hilfen wie ChatGPT oder SchulKI von OpenAI oder Gemini von Google zur Erstellung meiner Dissertation (Zutreffendes angekreuzt):

- ☐ Ich habe bei der Erstellung dieses Textes kein KI-Tool verwendet.
- ☒ Ich habe ein KI-Tool in den folgenden Bereichen eingesetzt (Mehrfachnennungen möglich):
  - ☐ Ideen finden, meine Kreativität anregen
  - ☐ Verstehen von Konzepten, Recherche von Fakten und Definitionen
  - ☒ Optimierung eines von mir verfassten Textes
  - ☐ Erstellen ganzer Textpassagen nach meinen Vorgaben

Folgende KI-Tools habe ich verwendet, damit aufgeführte Teile meines Textes von dem Tool wie folgt profitiert haben:

- Thesify: Ich habe die Endversion der Thesis von thesify analysieren lassen, um argumentative Schwachstellen zu finden, und um eine generelle Rückmeldung bezüglich Sprachqualität und Struktur zu erhalten.

Signed: _____

Date: _____

Abstract

The aim of this thesis was the development and characterization of a cold atmospheric plasma source (CAP) tailored for clinical applications. During experiments, various materials were tested in a long-term plasma afterglow environment for their suitability in CAP decontamination and as components for CAP sources, and afterwards a novel, adaptable CAP source was built and characterized. For the suitability-study, materials were chosen from different material groups, namely metals (stainless steel), glass (borosilicate glass) and polymers (polypropylene, rigid polyvinyl chloride and fluorinated ethylene propylene), representing typical materials used in the healthcare sector.
Here, different degrees of surface modification were found. While fluorinated ethylene propylene showed almost no modifications, slight to significant changes in free surface energy, surface morphology, surface composition and oxidation was found for the other materials, especially stainless steel. Additionally, sporicidal efficacy of the CAP source was proven, with a $\log_{10}$ reduction of *Bacillus atrophaeus* endospores of 4.3-6.2 within 15 minutes. Here, hydrophobic properties of the tested materials and hence layering and shielding of the bacteria showed the greatest limiting effect in spore reduction.
Based on these findings, the prototype of a CAP source was designed and constructed. Aim for this design was to create an adaptive, low-cost, efficient and durable plasma source. Hence, sputter-coating of the electrodes on a flexible dielectric material was tested. As dielectric, polyethylene naphthalate (PEN) foil was chosen because of its high dielectric strength and excellent chemical resistance. By sputter-coating, different electrode materials and electrode thicknesses were deposited onto the PEN foil and tested for their resistance against material modifications and for their endurance during plasma ignition. Based on its performance, palladium was chosen, with a thickness of 110 nm for both electrodes.
For this prototype (palladium-sputtered electrodes with thickness 110 nm on both sides), different characterization tests were done. Firstly, ozone measurements revealed plasma parameters for ozone and nitrogen mode. Secondly, laser microscopy showed the development of a border area on the edge of the grounded electrode. Thirdly, plasma diagnostical approaches indicated electron temperature, electron density and vibrational temperature for nitrogen mode, and plasma power was evaluated. Lastly, bactericidal efficacy was measured for different ozone mode plasma parameters and for nitrogen mode, using different CAP source prototypes. Here, within 5 minutes, a $\log_{10}$ reduction of 6.7 (nitrogen mode) and 5.3 (ozone mode) was achieved, respectively.
Endurance of the different plasma mode prototypes showed to differ, depending on the used plasma mode. While the nitrogen mode prototype burned through after almost 150 minutes, corresponding to 50 plasma ignitions, the two ozone mode prototypes still worked reliably after the end of the experiments.
An evaluation of the performance of the newly developed CAP prototype shows, that reduction efficacy is in the same order of magnitude, but with shorter required treatment intervals than the plasma source used during the material tests. At the

same time, the newly developed prototype works with an power density, which is one order of magnitude lower than that used for the previous plasma source, indicating improved effectiveness.
To sum it all up, the experimental studies conclude, that the treatment with cold atmospheric plasma is a non-destructive and adaptable cleaning method for various materials. Combining CAP treatment with conventional sterilization methods could enhance the pathogen reduction, especially with regard to geometrically complex or heat-sensitive materials. PEN foil as dielectric has promise because of its characteristics and sputter-coating technique shows to be an adaptable and low-cost possibility to produce flexible and highly effective cold atmospheric plasma sources.

Zusammenfassung

Das Ziel dieser Dissertation war die Konstruktion, Entwicklung und Charakterisierung einer kalten atmosphärischen Plasmaquelle (eng. Cold Atmospheric Plasma; kurz: CAP) für klinische Dekontaminationsanwendungen. In experimentellen Studien wurde eine Bewertung der Langzeitwirkung von kaltem Afterglow-Plasma auf verschiedene Materialien vorgenommen, um deren Eignung für die Plasmadekontamination zu bestimmen, und im Anschluss, basierend auf den Erkenntnissen der Langzeitstudie, eine neuartige, flexible CAP-Quelle gebaut. Die zu untersuchenden Materialien für die Langzeitstudie wurden aus drei Materialgruppen, welche im klinischen Alltag vertreten sind, gewählt. Hierbei handelte es sich um Metall (Edelstahl), Glas (Borosilikatglas) und Polymere (Polypropylen, weiches Polyvinylchlorid und Fluorethylenpropylen). Im Zuge von Oberflächenmodifikationsuntersuchungen zeigte sich, dass die Behandlung mit kaltem Plasma im Allgemeinen die Oberflächenbenetzbarkeit mit Flüssigkeiten, die Zusammensetzung der Oberflächenenergie und die Oberflächenmorphologie veränderte. Zudem wurden Veränderungen der chemischen Zusammensetzung der Oberfläche und Oxidation gefunden. In den Experimenten wies Edelstahl gegenüber den anderen getesteten Materialien die signifikantesten Modifikationen auf, während Fluorethylenpropylen durch die Plasmabehandlung praktisch nicht verändert wurde.
Mit Hilfe von *Bacillus atrophaeus* Endosporen wurde zudem die dekontaminierende Wirksamkeit der Plasmaquelle gezeigt, wobei je nach Material eine $\log_{10}$-Reduktion von 4,3-6,2 innerhalb von 15 Minuten erreicht werden konnte. Hierbei waren die hydrophoben Eigenschaften der verschiedenen Materialien und die sich daraus ergebende gegenseitige Abschirmung der übereinanderliegenden Bakteriensporen während der Plasmabehandlung der entscheidende limitierende Faktor, während ein Einfluss der Oberflächenmodifikationen nicht nachweisbar war.
Basierend auf diesen Erkenntnissen, wurde eine neuartige CAP-Quelle entwickelt, für die aufgrund seiner hohen dielektrischen Durchschlagsfestigkeit und herausragender chemischer Beständigkeit eine Folie aus Polyethylennaphthalat (PEN) als Dielektrikum genutzt wurde. Durch das Aufsputtern von Elektrodenmaterial auf die flexible Oberfläche der Folie wurde eine verformbare Plasmaquelle geschaffen. Hierbei wurden verschiedene Elektrodenmaterialien und -dicken auf ihre Plasmaresistenz getestet, wobei letztendlich Palladium mit einer Dicke von 110 nm verwendet wurde. Die mit diesen Eigenschaften hergestellte Plasmaquelle wurde im Folgenden mit Hilfe unterschiedlicher Analysemethoden charakterisiert.
Zunächst wurden die Plasmaparameter bestimmt, mit welchen die CAP-Quelle im reinen Ozon- und Stickstoffmodus betrieben werden konnte. Mit Hilfe von Plasma Diagnostik wurden zudem die Elektronentemperatur, -dichte und Vibrationstemperatur im Stickstoffmodus und die Leistung des Plasmas bestimmt. Mittels Lasermikroskopie wurde eine durch die Plasmabehandlung erzeugte Grenzfläche auf den Plasmaquellen sichtbar. Außerdem wurden die bakteriziden Eigenschaften mit Hilfe von *Escherichia coli* Bakterien gezeigt.
Dabei wurden Bakterienexperimente im Ozon- und Stickstoffmodus durchgeführt.

Hierbei zeigte sich, dass die höchste bakterizide Wirksamkeit im Stickstoffmodus erreicht wird, mit einem $\log_{10}$-Reduktionswert von durchschnittlich 6,7 innerhalb von 5 Minuten, wobei der hierfür verwendete Prototyp mit 50 Plasmazündungen in fast 150 Minuten Betriebszeit im Vergleich zu dem im Ozonmodus betriebenen, welche auch nach Abschluss der Experimente noch voll funktionsfähig waren, eine kürzere Lebensdauer aufwies. Im Vergleich dazu wurde mit den im Ozonmodus betriebenen Prototypen ein $\log_{10}$-Reduktionswert von bis zu 5,3 innerhalb von 5 Minuten erreicht.
Vergleicht man die Ergebnisse der beiden Studien, so wird deutlich, dass die Bakterienreduktion des neu entwickelten Prototypen vergleichbar ist mit der vorher verwendeten Plasmaquelle. Gleichzeitig benötigt die neu entwickelte Plasmaquelle für diese Ergebnisse kürzere Behandlungszeiten und eine um eine Größenordnung geringere Leistung, was insgesamt auf eine verbesserte Effektivität hindeutet.
Insgesamt erwies sich die CAP-Behandlung als eine erfolgreiche, nicht-destruktive Reinigungsmethode für eine breite Palette von Materialien, insbesondere für hitzeempfindliche Materialien oder komplexe Geometrien der zu behandelnden Oberfläche. Die Ergebnisse deuten darauf hin, dass CAP-Dekontamination als Ergänzung zu herkömmlichen Sterilisationsmethoden eingesetzt werden sollte, um die Reduktion von Krankheitserregern insgesamt zu erhöhen. Die Verwendung von PEN-Folie als Dielektrikum, genau wie die Methode des Elektrodenaufsputterns zur Herstellung flexibler, günstiger, effizienter und anpassbarer Plasmaquellen bietet sich hierbei an.

Acknowledgements

First I'd like to thank my supervisor Prof. Dr. Markus H. Thoma for providing me the opportunity to do my Ph.D. and his support throughout my time as a Ph.D. student.
I also would like to thank the rest of my thesis committee: Prof. Dr. Claudia Höhne, Prof. Dr. Anja Henss and apl. Prof. Dr. Jens Sören Lange.
The countless hours at university would not have been as fruitful and fun without my colleagues from AG Thoma. I would like to especially thank my colleagues Daniela Coenen and Alisa Schmidt for supporting my work in the laboratory and for joyful conversations during coffee breaks. Moreover, I want to thank Janosch J. Perlbach for his support in the laboratory during my pregnancy and Christian Schinz and Dr. Martin Becker for their advice and help for the realization of my plasma source prototype.
At last, but not at least, I want to thank my parents for supporting me throughout my studies, my kids for all the laughter and joy they are bringing to my life, and Dr. Roman Bergert for his continuous support throughout my thesis.

Contents

List of Figures

Chapter 1

Introduction

Millions of deaths every year are caused by hospital-acquired multidrug-resistant microbes [1, 2] and the increase in antibiotic-resistance leads to significantly longer hospital stays and higher healthcare costs [3]. A breakthrough in plasma physics in the beginning of the 21th century gave new perspective to the fight against microbes. Scientists discovered, that cold plasma at atmospheric pressure (CAP) was able to deactivate bacteria, fungi and viruses, on agar plates under laboratory conditions [4–8], but also on different surfaces [9, 10] and on human skin [11–13] without thermal or destructive stress for the surrounding cells of (human) tissue. Further research found even wound healing and cancer threatening interactions of plasma with cells [14–17]. This opened up a new field of plasma application, the so-called plasma medicine sector. Scientists from different backgrounds, namely physics, biology, medicine, chemistry and engineering united their knowledge and started to research to better understand the effects of plasma treatment.
Quickly it became apparent, that plasma treatment was not only effective with single, non-resistant bacteria, but also biofilms [18, 19] and antibiotic-resistant bacteria, such as Methicillin-resistant *Staphylococcus aureus* (MRSA) [12, 20–23], could be deactivated with CAP treatments. Heat sensitive surfaces, such as food [7] and human skin [12], could be treated and also plasma activation of water showed beneficial effects, e.g. in cancer treatment [24, 25]. As a consequence, other CAP application sectors, such as agriculture, nutrition science and chemical treatments arose [26].
In contrast to conventional cleaning methods, such as UV sterilization, the use of ethanol, or steam pressure sterilization [9, 27–29], plasma treatment acts quickly and can be used on temperature sensitive surfaces and, due to its gaseous nature, can even be used on difficult geometries or inaccessible surfaces such as capillaries [20, 30]. Moreover, no residues are left after plasma decontamination, and it provides an inexpensive alternative for the decontamination of spacecraft equipment [31]. Plasma for medical treatment is generated at lower input powers compared to plasma that is used for etching or in ozone generation reactors [32, 33].
Despite its lower input powers and low thermal temperature [26], CAP is highly reactive due to different reactive oxygen and nitrogen species (RONS), generated by the high energetic free electrons of the plasma [11, 34]. To achieve safe and reliable decontamination procedures, one has to take into account the materials' characteristics after multiple decontamination processes, for treated material samples as well as for the plasma setup materials. While different research groups investigated activation and modifications of surfaces directly after plasma treatments [35–42], as well as recovery processes of surface modifications within up to 5 days after plasma treatment [41], the long-term influence of plasma decontamination on different materials was not tested yet. Especially a comparative study on different material groups with one plasma source, and on the effect of multiple plasma decontamination processes simulating long-term use was missing. Hence, in a first experimental series, the

influence of CAP treatment on different materials, commonly used in the medical sector, was tested [43]. Using the results of the first experimental setup and given the fact, that the used plasma source regularly needed to be polished and the conjunctions to be renewed due to chemical reactions of the used materials, a novel plasma source was designed.
Here, focus was set to find electrode and dielectric materials, that met the requirements of being chemically stable during and after plasma ignition. At the same time, a plasma geometry had to be found where a maximal reaction output could be generated. The novel plasma source was characterized for different plasma modes, to achieve an adjustable mix of reactive species and thus a broad and diverse spectrum of application. Another characteristic that was met was the adaptability to different treatment geometries, hence a small and flexible plasma source, that worked without external gas inlet, was built and characterized [44].

To meet the requirements of medical decontamination, *Bacillus atrophaeus* endospores and *Escherichia coli* bacteria respectively were used to verify bactericidal and sporicidal efficacy of the two plasma sources in the experiments.

In the following chapter, an overview of the most important aspects of CAP, such as possible technical realizations, significant plasma properties, and the subsequent deactivation mechanism on living cells is given. Physical and biological methods to achieve the results presented in the publications are explained in detail in the sections 2.2 and 2.4. In addition, a brief overview is given of the physical, chemical and biological methods used to characterize the CAP itself and its effects on living cells. A deeper insight will be given to each publication in chapter 3, followed by the corresponding articles in chapter 4 and 5. At the end, the findings of the two articles will be placed in the context of their medical use and an outlook for future application will be given.

Chapter 2

Background Information

2.1 Overview of cold atmospheric plasma physics

Plasma, named by Irving Langmuir with the Ancient Greek word for "moldable substance", can roughly be described as an ionized gas. Typically, plasmas are defined as the fourth state of matter as they can be generated by increasing the energy of gaseous systems. Through the increase of energy, free electrons and ions are generated, hence plasmas are electrically conductive, one of the main characteristics of plasma in contrast to systems in the gaseous state. Depending on the type of discharge and the environment, plasma can have different degrees of ionization, different proportions of neutral gas in the ionic state, and different energetic states of molecules and atoms.
In contrast to the phase transitions between solid, liquid and gaseous, the phase transition between gaseous and plasma is rather smooth, and hence, depending on the phenomenon, already ionized gasses with small degrees of ionization $<< 1$ can be described as plasma.
Most visible matter in the universe (more than 99% [45]) is in plasma state, e.g. stars and ionizing radiation. Plasma can be generated in different forms and using different physical techniques. Applications of plasma are as diverse as plasma's characteristics. There are many established plasma applications for industrial processes, often using either vacuum or a specific type of environment to produce, for example, thin functional layers. A very specific and emerging area that is not yet established in industry is the ignition and use of plasma in the atmosphere and on living cells and tissues.
This new field of application for weakly ionized plasma, is the so-called field of plasma medicine, where the mixture of different species produced is used to obtain different interactions with the surrounding chemical, for example to help clean and regenerate a chronic wound. Here, the reactive outcome of physical plasma with the surrounding air or gas is used to inactivate bacteria, fungi and viruses on surfaces and in wounds, to enhance wound healing and to destroy cancer cells. Moreover, the characteristics of plasma to inactivate pathogens were further transmitted to the fields of agriculture and food technology and hence, there is a wide field of research now as well.
One strong advantage of weakly ionized plasma is the rather non-damaging characteristic and, strongly linked to that, the fact that it can be generated at low temperatures, namely close to room temperature. The reason for this unique characteristic is the difference in mass of electrons, ions and neutral gas components. While ions and neutral gas atoms with their relatively huge mass (compared to electrons) hardly get accelerated by the time of one discharge cycle and are thus low-energetic with energies in the order of $1/40\ eV$ ($\approx$ 290 K or 17 °C), the lighter electrons get accelerated and thus have energies in the order of $1eV$. Hence, the plasma is in non-equilibrium.

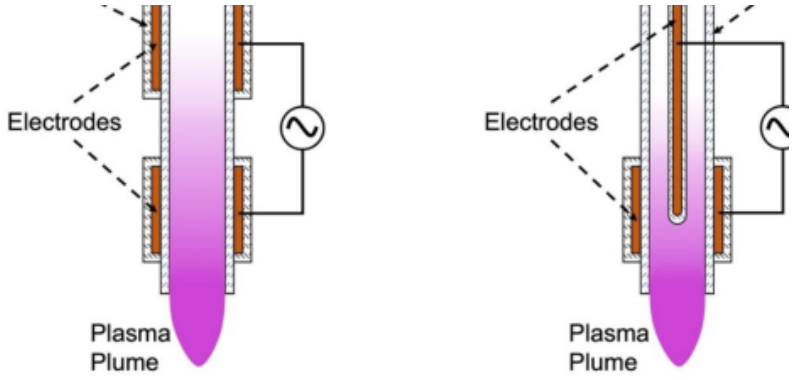

FIGURE 2.1: Different plasma jet configurations typically used in plasma medicine. Adapted from [47].

Due to the small mass of the electrons, there is only a small energy transfer when colliding with for example the skin, while the noticeable temperature of the plasma is dominated by the energy transfer of the ions and neutral gas components.
Using different techniques, these low temperature plasmas can be generated at low pressure using a carrier gas, such as argon (Ar), helium (He) or xenon (Xe)[16], or at atmospheric pressure where molecules of the surrounding gas, in most applications the air itself, are ionized [18, 20].

2.1.1 Cold Atmospheric Plasma Sources

These plasmas, so-called "cold atmospheric plasma"(CAP), can roughly be divided into two groups, depending on the plasma geometry. Firstly, CAP can be generated as a jet-configuration, where inside of an insulator or dielectric a plasma is generated between two electrodes and the plasma is extruded due to the active gas flow regulation as a plume through a nozzle (compare figure 2.1). One characteristic of this first group - the CAP jets - is the need of carrier gasses and the small plasma geometry, which results in highly accurate plasma treatments of small treatment areas due to the plume's sharp and roughly linear outcome. One possible application for CAP jets is the treatment of root canals, where precise and fine treatment is necessary [46].

Secondly, plasma can be generated as a dielectrical barrier discharge (DBD), which in contrast to jet plasmas has a wider geometry and a rather diffuse plasma outcome. The group of DBD plasmas again can be devided into three subcategories. Here, volume DBD plasmas, floating electrode DBD, and surface microdischarge plasmas (SMD plasmas).
The differences between floating electrode DBD, volume DBD and SMD plasma can be seen in figure 2.2. While all DBD-types consist of a driven electrode and a dielectric, volume DBD and SMD plasmas have a second, grounded electrode, whereas floating electrode DBDs use the treatment target as grounded electrode.
The major difference of volume DBD and SMD plasma sources is the position of the grounded electrode. While for volume DBD plasmas there is a gap between driven and grounded electrode (each possibly in contact with the dielectric), which could be filled with a carrier gas or with air, the driven and grounded electrodes are directly attached to one dielectric for SMD plasma configurations. As a consequence, samples in a floating electrode DBD or volume DBD setup can be directly exposed to the generated plasma by placing them in the gap between driven and grounded electrode or by using the sample as grounded electrode. Hence, a high range of short-

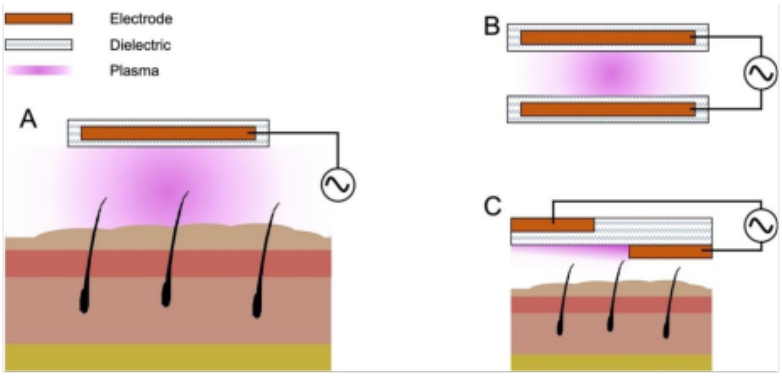

FIGURE 2.2: Different DBD plasma setups. **A** shows a Floating Electrode DBD, **B** a Volume DBD and **C** an SMD plasma source. Adapted from [47].

and long-living species, generated by the interaction of plasma with the surrounding gas can interact with the sample. These species are highly reactive and consist - for air as carrier gas - mainly of different reactive oxygen and nitrogen species (RONS). In contrast to this, plasma-gas interaction, and hence the emitted light of the plasma, is localized at the borders of the grounded electrode for SMD plasmas. Here, to improve the production of RONS, the grounded electrode has a grid-like configuration to maximize the total electrode border area. At this border, gas molecules get chemically excited by the reaction with the free electrodes in the plasma. As a consequence, reactive species develop, which further react with other gas molecules in the plasma chamber. The dispersion of activated gas molecules continues until the entire experimental chamber is filled with reactive species, but in contrast to floating electrode DBD and volume DBD devices, only long-living species with a lifetime of more than a few seconds reach the target and thus are relevant. This gaseous mixture is described as plasma afterglow [48]. In afterglow plasma sources, there is no current transfer from the plasma to the target [49].
Experiments presented in this thesis were based on different SMD plasma sources, thus the generation mechanism of dielectrical barrier discharge plasmas is described in more detail in the following section.

Dielectrical Barrier Discharge Plasma Generation

At atmospheric pressure, plasma is generated by high electric fields. As soon as a configuration-specific voltage and frequency is reached, free electrons are accelerated between the electrodes, which leads to an electrode avalanche, and finally an arc discharge towards the grounded electrode is generated. To suppress the arc discharge, a dielectric barrier is added between the two electrodes. Hence, after the start of the electrode avalanche, the electrodes accumulate on the dielectric and the electric field strength is reduced. In direct current conditions (DC), the ions in the electrode gap stream towards the cathode and the plasma discharge stops. Those streams, so-called filaments, have a lifetime in the order of nanoseconds. By combining this process with an alternating current (AC), the frequency can be chosen in such an order of magnitude (often in the range of kHz) that the ions, which are a lot slower than the electrodes, do not have enough time to stream towards the cathode and hence the formation of filaments is suppressed. This phenomenon is called ion trapping. The separation of electrons and ions by their inertia leads to a correlation

between external frequency, collision frequency, applied voltage and the distance between the two electrodes. Hence, by carefully choosing a suitable dielectric, stable plasma discharge with suppressed filaments can be realized.[50]
During these processes, free electrons and ions of the plasma interact and chemically react with the surrounding air close to the electrode. Air molecules get excited, charged or ionized and different reactive species, such as O_2^*, N_2^*, $^{\cdot}O_2^-$, N_2^+, $^{\cdot}OH$, $O^{\cdot}$, $^1O_2$, NO_X, H_2O_2 and O_3 [11, 24, 34] are produced.
For floating electrode DBDs and volume DBDs, all these reactive species interact with the treatment target, varied in concentration depending on the environmental conditions. In contrast to this, SMD devices have a distance between the ignited plasma at the interface of grounded electrode and dielectric, and the treatment target, hence not all of these reactive species are able to reach the target. The reactive species further interact and react with the surrounding air, and the radicals (short-living species) [51] react to neutral molecules, which are the long-living species, and hence dominate the plasma afterglow, which is prominent in the treatment chamber. Bacteria or material samples, placed underneath the SMD plasma source, interact with these long-living reactive species.
During the experiments, different bacteria were plasma-treated with different SMD plasma sources. Hence, a brief introduction to bacterial experiments and plasma-bacterial interactions is given in the following section.

2.2 Terms and Concepts of Bacterial Experiments

The term "bacteria", often used as a definition of small organisms in general, is rather unspecific. Bacteria can be divided into different groups, depending on characteristics like cell wall structure, shape, host-environment, or nutrient intake. In fact, we humans are closer related to any plant, regarding the structure of our cells, than some bacteria belonging to different bacteria families are to each other [52, 53]. All life forms are classified into three domains, namely bacteria, eucarya, and archaea [54]. Bacteria and archaea are organisms made of prokaryotic cells, which means that their DNA is not embedded into a nucleus but forms a nucleoid in the cell's cytoplasm, while eucarya are organisms made of eukaryotic cells (as plants, animals and humans) and hence their cells have a nucleus surrounding the DNA strain.
CAP treatment with both bacteria and eucarya has been researched intensively and the treatment with heat, shear stress or UV light, as well as the reaction with reactive oxygen and nitrogen species and charged species was found to cause effects in the cell's viability. Usually, CAP sources are designed to limit UV emission, shear stress and thermal damage, for they need to meet the requirements of treating living tissue. As a consequence, the production of charged particles (not for afterglow plasma) and RONS is found to be the underlying mechanism of cold atmospheric plasma treatment. The effects of CAP on eukaryotic and prokaryotic cells can be lethal and nonlethal, but considering the more advanced defense system and the much better repair possibilities of eukaryotic cells, higher treatment doses are required to induce lethal effects in eukaryotic cells than in prokaryotic cells. Hence, plasma treatment can be adapted to cause lethal effects selectively in prokaryotic cells. [49]
The group of bacteria can be further divided, describing different characteristics of bacteria groups. One important criterion is the classification as to whether the bacteria is gram-positive or gram-negative. Here, various bacteria react differently on Gram staining, depending on the structure of their cell wall. While gram-positive

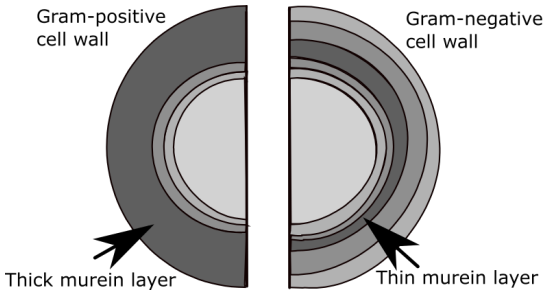

FIGURE 2.3: Differences of cell wall structure for gram-positive and gram-negative prokaryotes, adapted from Roland Mattern [57].

bacteria, such as bacteria of the genus streptococcus, enterococcus or bacillus, have a thick layer of murein in the cell wall, gram-negative cells, such as the family of enterobacteriales, have a thinner murein layer. [55, 56]
In figure 2.3, the differences in cell wall structure of gram-positive and gram-negative bacteria can be seen. Given the context of bacteria inactivation, which is the target of plasma medical applications, research groups tested the resistance of gram-positive and gram-negative bacteria to different plasma treatments [20, 58]. Laroussi *et al* [59] found for example, that with their plasma source the inactivation of gram-positive *Bacillus subtilis* and gram-negative *Escherichia coli* was possible, but furthermore found the cell walls of the gram-negative bacteria to be destroyed, while the gram-positive bacteria's cell wall was rather intact. Naturally, bacteria have developed certain mechanism to prevent themselves from outer stress. As a consequence, some bacteria are able to form biofilms, a syntrophic community of microorganisms, to build a bacteria matrix with inner matrix communication and different functions inside the matrix [60]. Other bacteria are able to form endospores, which means they are, if conditions are unfavorable, in a state comparable to winter dormancy, and hence capable of reaching a high degree of resistance [61]. Different research groups found both biofilm forming and spore forming bacteria to be sensitive and prone to CAP treatment [43, 62–66], and - combining the characteristics of biofilm forming and differences in cell wall structure - Mai-Prochnow *et al* [58] found gram-negative biofilms to be more sensitive to plasma treatment than gram-positive biofilms.

2.2.1 Bacteria sample preparation

For the experiments, two different bacteria strains were used and hence, different sample preparation was necessary. During the experiments, presented in chapter 4, *Bacillus atrophaeus* NRS 1221A endospores were used, for those presented in chapter 5, *Escherichia coli* K12 MG1655 was used. The following subsections will clarify some important microbiological terms, to introduce the two bacteria strains and to describe sample preparation for the two cases.

Microbiological Terms

To understand bacteria sample preparation, one needs to understand some terms of microbiology first. Therefore, the most important measurement and preparation techniques, terms and definitions are explained briefly in the following enumeration:

Agar Plates are petri dishes, filled with a gelatin-like substance called agar-agar. The agar is further mixed with different nutrients which encourage bacteria growth.

Culture Medium is a liquid or agar containing different substances for optimal bacteria growth. Depending on the bacteria species, different culture media are available. During the experiments, lysogeny broth (LB) was used for the cultivation of *Escherichia coli* and R2A for the cultivation of *Bacillus atrophaeus*.

Incubation is the term used for bacteria growth under ideal temperature conditions. Here, either a bacteria solution or an agar plate with bacteria plated on it is placed for a specific time (usually 24-48 hours) inside the incubator and temperature is set to a fixed value, depending on the bacteria. During the experiments, *Bacillus atrophaeus* were incubated at 32 °C, *Escherichia coli* at 37 °C.

Cell forming units (CFU) describes the number of bacteria, that are able to reproduce after a treatment. To evaluate the number of CFU, agar plates with the bacteria suspension equally spread on, are incubated after cold atmospheric plasma treatment. Through incubation, every reproducible bacteria forms an individual colony which is visible on agar as a small dot, hence the total number on the plates can be counted and compared to an untreated sample, the so-called 'reference sample'.

Vortexing describes the process of mixing a liquid medium with bacteria to create a homogeneous dilution of the bacteria culture. Here, a special mixer, the so-called 'vortexer', is used.

Plating is the process of applying a bacteria suspension onto the agar plate. One method to plate is by pipetting a specific amount of the suspension onto the agar and then spreading out the suspension homogeneously with a sterile Drigalski spreader.

Dilution Series describes a mechanism, where high-concentrated bacteria suspensions are diluted in several steps to get a countable bacteria concentration in reference samples. Usually, bacteria concentration is reduced by one $\log_{10}$ with every dilution step.

Optical Density is a value that describes the opacity of bacteria solutions. The densitometer is tared to the optical density of 1000 μl of the used culture medium inside a glass cuvette and then the optical density of 1000 μl of the bacteria solution in the culture medium inside a glass cuvette is measured. By dilution of the bacteria suspension, the optical density of the suspension is adjusted to a fixed value, hence the bacteria solution contains the same amount of bacteria for every experimental procedure. One has to take into account, that optical density measurements do not differentiate between living and dead bacteria, thus the bacteria solution has to have the same age and has to be stored at known conditions, especially regarding the temperature, for every procedure.

D-value describes the treatment time that is necessary to achieve 1 $\log_{10}$ reduction of bacteria.

Log $_{10}$ Reduction	Reduction of Bacteria [%]	Surviving Bacteria out of 100.000.000
1	90	10.000.000
2	99	1.000.000
3	99,9	100.000
4	99,99	10.000
5	99,999	1.000
6	99,9999	100
7	99,99999	10
8	99,999999	1

TABLE 2.1: Number of surviving bacteria for different log reduction values. Adapted from [67].

Decontamination and Sterilization are two terms, strongly linked to each other. While decontamination describes in general the removal and reduction of microorganisms such as bacteria, viruses, spores and fungi, sterilization describes the complete deactivation of all forms of life. As sterilization can not be proceeded with 100% accuracy, usually a certain $\log_{10}$ reduction and hence only a decontamination is achieved in reality. In table 2.1, the $\log_{10}$ reduction stages are opposed to the corresponding percentage of inactivated bacteria and the corresponding number of surviving bacteria. Here, for example a $\log_{10}$ reduction of 6 needs to be achieved for clinical operation equipment [67] and from $\log_{10}$ 5 the decontamination is described as high-level disinfection [68].

Statistically Valid Results are achieved by replication of the experiments. Here, the experiments were conducted at least three times on different days to ensure that the results are consistent and reliable.

Bacillus atrophaeus

Bacillus atrophaeus (*B. atrophaeus*) is a gram-positive, rod-shaped bacteria which naturally hosts in soil [69]. Cells form at aerobic conditions e.g. on R2A agar in a temperature range from approximately 5°C to 55°C, where the optimal conditions are between 28-33°C [70, 71]. Under harsh conditions, they form endospores. *B. atrophaeus* was established as industrial bacterium, among others to verify disinfection agents, in studies of biodefense, and as sterilization indicator [69, 72].
For bacteria sample preparation, a master suspension with a bacteria density of approximately 10^8/ml of *Bacillus atrophaeus* NRS 1221A endospores, dissolved in deionized water, were used. First, a defined droplet of the master suspension was spread on the material samples and dried over night. Afterwards, the samples were plasma-treated for different treatment times. After that, the samples were added to deionized water, and vortexing and ultrasonic treatment were used to suspend the bacteria again in water. Using this plasma-treated suspension, a dilution series was conducted and finally the diluted suspension was spread on R2A agar plates. To evaluate the cell's ability to form new cells, these agar plates were incubated and the cell forming units were counted the following day.
In contrast to this experimental setup using bacteria endospores, *Escherichia coli* K12 MG1655, used for the experiments in chapter 5, were treated differently.

Escherichia coli

Escherichia coli (*E. coli*) is a gram-negative, rod-shaped bacterium which is found in the human microbiome [73]. *E. coli* has lots of different strains, most of them harmless, but some of them pathogenic, e.g. enterohemorrhagic *E. coli* (*EHEC*). It has been investigated intensively and nowadays is an important prokaryotic model organism in microbiology [74–77].
For bacteria sample preparation, one *E. coli* colony was taken with an inoculation loop from the pure microbial *E. coli* K12 MG1655 culture on LB agar in the fridge and was diluted into liquid LB medium. The tube containing the LB-bacteria-solution was stored over night at 37 °C in the incubator, slightly shaking the tube with the help of an orbital shaker.
The following day, the bacteria concentration of the suspension was standardized, using optical density measurement technique. On average, a bacteria density of 5.75 $\cdot 10^8$/ml was reached. For plasma treatment, the bacteria solution was spread on LB agar plates, which were incubated after plasma treatment, and the number of cell forming units was counted the following day.
To analyze the inactivation of bacteria, two different cold atmospheric plasma sources were used, which are presented in the following section.

2.3 Experimental Design, Materials and Set-up

2.3.1 Plasma Source I: Surface Micro-discharge chamber

The experiments to evaluate surface modification caused by cold atmospheric plasma treatment (see chapter 4) were conducted using an adapted surface micro-discharge plasma source, initially built by the Max-Planck-Institute Garching and its spin-off, the company terraplasma GmbH. In figure 2.4 a picture of the plasma source and the emitted light can be found, in figure 2.5 a sketch of the setup of the plasma source and the electric circuit of the experiments can be seen in detail. The SMD plasma setup consists of a driven copper electrode, a grounded aluminum grid, and a dielectric sandwiched between them. The whole setup, connected to a voltage amplifier for plasma generation, is at the top inside of a small box. For the experiments the box material was changed to PEEK due to erosion of the former material. The initial dielectric material was a 650 μm-sheet of polytetrafluoroethylene (PTFE), which was changed to quartz glass with a thickness of 1 mm.
A sinusoidal voltage of 9 kV_{pp} and a frequency of 2 kHz was applied to generate the plasma. Samples were placed at the bottom of the box on a grounded metal plate underneath the plasma source, with a distance of about 26 mm.
While the plasma discharge with this SMD plasma source was quite stable, a gradient of brightness of the discharge was visible with the brightest part being in the center of the plasma source and less bright at the corners. Hence, scaling of the discharge area would be limited. Furthermore, quartz glass as dielectric was stable in terms of burn through, which was a regular phenomenon for the PTFE sheets, but as material quartz glass is quite brittle and fragile, thus no versatile geometry could be achieved. In addition, erosion of the surrounding box material still occurred, as well as at the soldering points. A regular cleaning and renewing of the soldering points was necessary to achieve consistent results. As a consequence, novel dielectric material and electrode approaches were tested in the following experimental series.

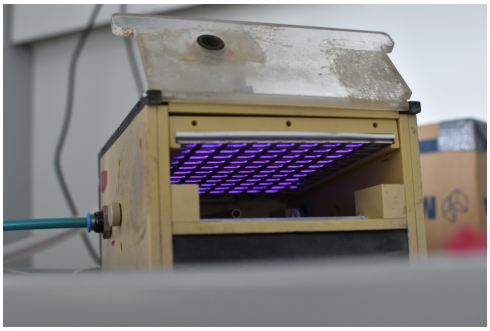

FIGURE 2.4: Picture of the SMD plasma chamber discharge.

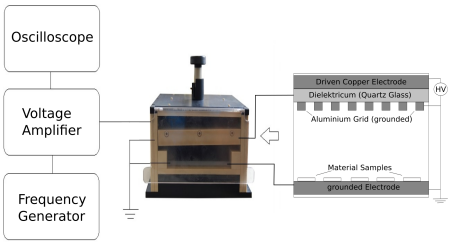

FIGURE 2.5: Sketch of the SMD plasma setup and electric circuit. Adapted from [43]

2.3.2 Plasma Source II: Flexible Sputter-coated Air DBD

These tests resulted in a flexible SMD plasma source with electrode material directly sputtered onto the dielectric material. The growth of these thin metal films was done using ion-beam sputter deposition on an in-house constructed system [78].
After probing different electrode materials and thicknesses (see chapter 5), palladium with a thickness of 110 nm for both electrodes showed best results in discharge stability. Here, the driven electrode had a square geometry, while the grounded electrode, where the plasma is generated, had a spiral geometry, to provide maximum edge area and hence - as described in section 2.1.1 - maximal reactive plasma outcome. Pictures, taken of the electrodes, can be seen in figure 2.6 and 2.7. As dielectric, polyethylene naphthalate-foil (PEN) with a thickness of 250 μm was used. The electrodes were contacted via screw joint, using plastic screws (see figure 2.6). Discharge parameter during experiments varied between 5.5 and 8.5 kV_{pp} and between 3 and 5 kHz. The material PEN was chosen, because of its promising characteristics. With a dielectric strength of 116 kV/mm, an electrical continuous use temperature of 180 °C and an excellent chemical resistance [79, 80], combined with a suitable dielectric constant, and with its flexible characteristics, PEN foil fulfilled multiple requirements to act as dielectric in a cold atmospheric plasma source. Moreover, the material tests in the first experimental series (chapter 4) showed a general tendency for polymers to be less affected by the plasma afterglow than the other test materials, hence the use of a polymer with appropriate characteristics was the next logical step in building a new plasma source. As this plasma source concept was only built as a prototype, cases had to be built to be able to conduct experiments. As a consequence, one case for plasma diagnostical measurements and one for bacterial experiments was built by 3D printing, using acrylonitrile styrene acrylate (ASA) as printing material. A sketch of those two experimental setups is shown in figure 2.8.
Apart from biological experiments as described in section 2.2, different experiments to analyze the plasma-treated surfaces, the plasma gas composition and afterglow properties were conducted, which will be described in the following section.

2.4 Analytical techniques for experiment evaluation

To evaluate the experimental outcome, different evaluation methods, adapted to the experimental requirements were needed. Here, a differentiation between the characterization of plasma and the analysis of treated surfaces was necessary.

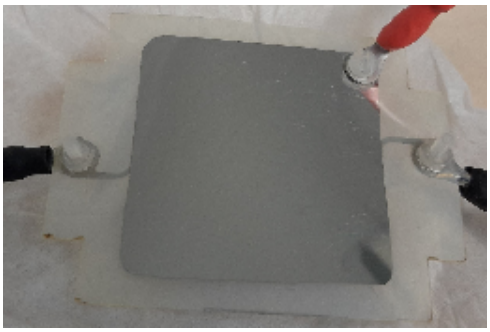

FIGURE 2.6: Picture of the driven electrode of the sputter-coated DBD prototype. Note, that the connections were realized using plastic screws. [44]

FIGURE 2.7: Picture of the plasma light at the grounded electrode of the sputter-coated DBD prototype. A homogeneous plasma discharge is visible. [44]

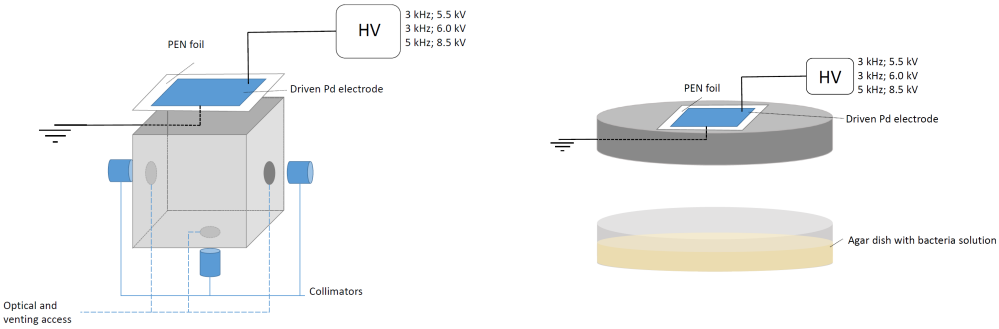

FIGURE 2.8: Experimental setups for plasma diagnostical and bacterial experiments. Adapted from [44]

2.4.1 Surface modification analysis

A central aspect of the experiments, presented in the publication in chapter 4, was the evaluation of surface modifications, caused by the cold atmospheric plasma treatment. But also in the second publication (Chapter 5), an analysis of the plasma source prototype's surface was executed to evaluate the dielectric material's characteristics and possible changes of the dielectric after plasma ignition.

Laser Microscopy

To provide a topographic scan of the materials' surfaces (be it of plasma-treated materials or the surface of the dielectric material) and to specify the surfaces' roughness before and after plasma treatment, laser microscopy with a wavelength of 408 nm, and 20x- and 50x-fold magnification was used. Here, the Keyence VK-9710 microscope and the Keyence VK Analyzer were used to evaluate the results.
For analysis, three samples of each material (plasma-treated and untreated), and accordingly three points of each sputter-coated plasma source were scanned and compared.
Further surface analysis, as described in the followig paragraphs, was only conducted for the material analysis of long-term plasma-treated materials (Chapter 4),

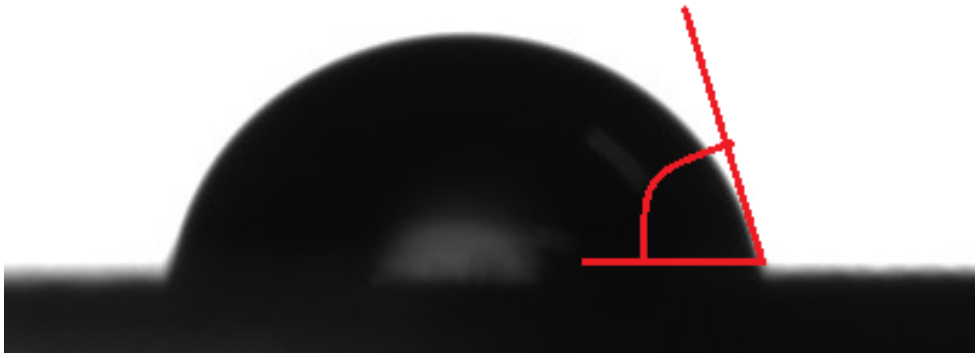

FIGURE 2.9: Contact Angle Measurement of liquid-solid interface.

while for the sputter-coated plasma source prototype the focus was set on the characterization of the generated plasma.

Contact Angle Measurements

After laser microscopy analysis, plasma-treated materials were tested for a change in their free surface energy, namely the polar and disperse fractions of the free surface energy. Therefore, contact angle measurements with the sessile drop method [81] with deionized water, ethanol, diiodomethane and ethylene glycol as reference fluids were performed and evaluated, using the OWRK-model [82–84]. The free surface energies of the reference fluids were taken from Ström *et al* [85] and Ohm *et al* [86].
To follow the OWRK-model, a droplet of the reference fluids, which had a defined volume, was extruded on the surface of the tested material sample. A picture of this droplet was taken and the contact angles for the different reference fluids at the liquid-solid interface were measured and compared. An example of this can be found in figure 2.9. Using the known polar and disperse fractions of free surface energy of at least two reference fluids, the polar and disperse fractions and the free surface energy of the samples can be calculated by comparing the contact angles.

X-ray Photoelectron Spectroscopy

As a third analysis method, X-ray photoelectron spectroscopy (XPS) was used to identify possible surface material composition changes due to plasma treatment.
XP-spectroscopy is based on the principle, that photoelectrons are emitted from surface molecules (surface layers of 1-5 nm) when they are treated with electromagnetic radiation. Depending on the energy of the emitted photoelectrons, they can be correlated to the atom and the orbital they belonged to [87] and hence, the spectra provides information, whether or not chemical surface modifications caused by the plasma treatment occured. Please note, that the settings used for the XPS analysis are described in detail in the publication (chapter 4).

2.4.2 Plasma Source Analysis

In addition to the surface analysis methods described in the previous section, also the gas of the plasma afterglow and the light emitted by the plasma were analyzed to get a deeper understanding of the characteristics of the probed plasma sources.

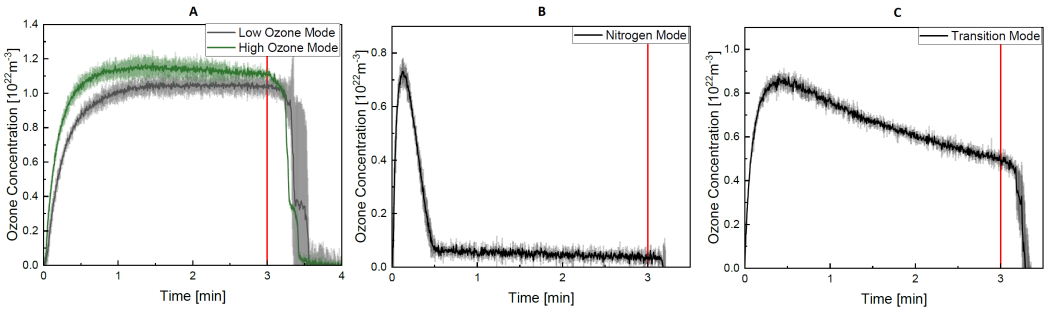

FIGURE 2.10: Spectrum of ozone concentration for different plasma modes. **A** shows the development of ozone until it reaches a plateau-value for pure ozone mode. In **B**, the increase and decrease of ozone concentration in pure NO_X mode is visible. Figure **C** shows transition mode, where in the beginning a high ozone concentration is reached. But instead of staying at a constant plateau-level, ozone concentration starts to decrease slowly over time.

Ozone Concentration Measurements

Medical plasma treatment can roughly be divided into two categories. First, there is the low-energy mode, the so-called "ozone mode", where interactions with radical oxygen species are dominant in inactivating prokaryotic cells. The second mode is the high-energy mode, or "nitrogen (NO_X) mode". Here, mainly reactive nitrogen species interact with the sample. Between the voltage and frequency parameters to run the plasma source in a "pure" high- or low-energy mode, there is a transition phase, where neither a pure ozone nor a pure NO_X mode can be achieved (compare figure 2.10). This transition from ozone to NO_X mode is caused by quenching reactions of ozone with nitrogen oxides, which are created at higher energy levels by the reaction of vibrationally excited nitrogen molecules with oxygen atoms [88]. As a consequence, a decrease in the concentration of ozone and simultaneously the increase of NO_X concentration can be observed.
To characterize plasma sources, and to determine experimental plasma input power and input frequency, ozone concentration measurements provide information about the ozone generation over time and hence the plasma setting parameters to run the plasma source either in ozone mode or in NO_X mode.
The physical principle this method is based on, is the absorption of light by gasses. Here, the light of a reference light source (UV deuterium lamp) is absorbed partly and characteristically by different gas molecules. An example of this phenomenon is Earth's atmosphere, where parts of the sun's light spectrum are absorbed. In medical plasma experiments, the absorption of light with a wavelength of 254 nm - as a marker for ozone concentration - is observed. Using Beer-Lambert law with an ozone absorption cross section of 1.1×10^{21} m^2 [89], the increase and decrease of ozone concentration relative to the initial ozone concentration in air can be calculated.

Plasma Diagnostics

Further analysis to characterize the two plasma sources were done by using plasma diagnostical approaches.
Plasma power and hence power density for both experimental setups were measured by evaluating the Lissajous curve of the plasma setup. Here, plasma voltage

and charge were measured, using an additional measurement capacitor (see figure 2.11). Afterwards, plasma power was estimated by integrating over the Lissajous curve (see figure 2.12) [90].

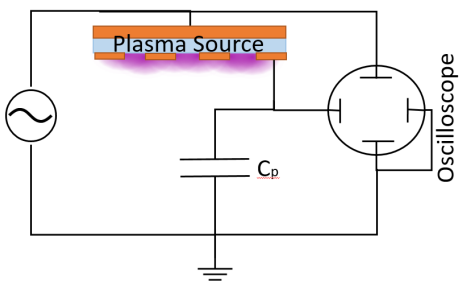

FIGURE 2.11: Setup to measure power density.

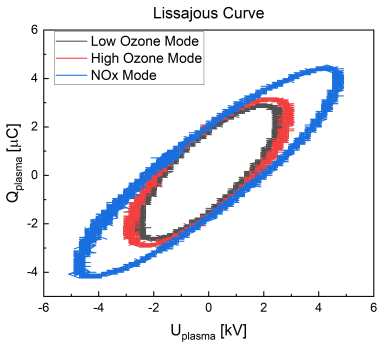

FIGURE 2.12: Lissajous curve for the three prototypes.

Furthermore, for NO_X mode of the sputter-coated plasma source (chapter 5), electron temperature, electron density and vibrational temperature of the plasma could be determined using the line ratio of nitrogen first negative and second positive system according to Fatima *et al* [91]. For ozone mode, in the measured spectrum the peak of nitrogen first negative and second positive system was not distinguishable from the background measurement, because nitrogen excitation is suppressed and power density and temperature are too low to generate a significant signal in ozone mode. As a consequence, these plasma parameter could not be calculated for ozone mode.

Chapter 3

Review of Published Articles

3.1 Surface modifications caused by cold atmospheric plasma sterilization treatment (Publication I)

Despite its low thermal temperature, plasma transfers high energy to the treated surface, and surface activation or etching mechanisms of different materials were found after plasma treatment by different researchers [35–42]. These results were obtained directly after short CAP treatments of 30 s to 90 minutes of the respective material. Still, a long-term study to investigate plasma-surface interaction with multiple plasma treatments and with a comparison of surface effects on different material categories was missing. Moreover, different research groups found the effects of surface modifications weakening over time due to recovery processes [40–42]. Hence, in the first experimental series, different materials, namely borosilicate glass, stainless steel AISI 321, and three different polymers (polypropylene (PP), rigid polyvinyl chloride (UPVC) and fluorinated ethylene propylene (FEP)) were plasma-treated with a SMD plasma source (compare section 2.3.1 and figure 2.5) in intervals of 30 minutes with at least 10 minutes breaks in between for 16 hours, to simulate a regular, long-term cleaning by plasma deactivation of these materials. Plasma parameters were set to reach ozone mode, with a power density of $130\frac{mW}{cm^2}$. Ozone measurements revealed, that the first 5 minutes were necessary for the plasma afterglow to propagate in the volume of the plasma chamber, whereas from minute 5 on, a stable ozone concentration was reached. Afterwards, the effect of plasma afterglow species on the materials' surfaces was investigated, using different analysis methods, namely laser microscopy, contact angle measurements and x-ray photo-electron spectroscopy. To eliminate unreliable results due to recovery processes as mentioned above, the surface analysis experiments were done at least 4 weeks after long-term plasma treatment.
Simultaneously, bacteria deactivation capability of the used plasma source was proven using *B. atrophaeus* endospores and treatment times of 5 to 15 minutes. Experiments were performed at least thrice to achieve reliable results. These results were corresponding to the measurements of ozone concentration, and bactericidal effects were found to be strong from the fifth minute until the fifteenth, and rather weak during the first 5 minutes. Results showed an averaged $\log_{10}$ reduction of the spore count between 4.3 and 6.2 within 15 minutes for the different materials, with a detection limit between 6.2 and 6.8, depending on the material. The area on the material sample, filled with the bacteria suspension droplet, and as a consequence an increased risk of stacking and shielding mechanisms were assumed to be the strongest limiting factor of bacteria inactivation.
During surface analysis, different kinds and degrees of surface modifications were found to occur. Here, oxidation and slight etching processes, as well as a change of

the material's free surface energy and, as a consequence, changes of the polar and disperse fractions of the surface energy were found. The greatest effects were visible on stainless steel, whereas borosilicate glass and the different polymers showed only slight modifications. Especially FEP has to be emphasized, as after long-term plasma treatment, only modifications within the error range occurred.
To summarize the results found during the first experimental series, different surface modifications were found to be caused by long-term plasma treatment of 16 hours in total, with its effects measurable even 4 weeks after treatment. At the same time, most of the long-term effects that could be found were nondestructive, and hence for normal disinfection treatment of surfaces negligible - for some applications the change in wettability could even be favorable [28]- but nevertheless the influence of plasma treatment on different materials has to be taken into consideration when choosing the appropriate cleaning technique. As a consequence, plasma treatment was found to be less favorable for the cleaning of metals and other materials prone to oxidation but showed at the same time to be highly effective for bacteria deactivation on glass and polymer surfaces. As a further finding of this first experimental series, materials for plasma sources (electrode, dielectric and case material) have to be chosen carefully, to generate safe, reliable and long-living plasma sources.

3.2 Characterization of sputter-coated polyethylene naphthalate-foil as novel flexible surface DBD plasma source (Publication II)

Using the results of the surface modification study [43], the prototype of an air DBD plasma source was built, combining the process of sputter-coating and the excellent chemical characteristics and resistances of a thin polymer foil made of polyethylene naphthalate (PEN). Here, PEN foil was used as a dielectric. Due to its thickness of only 250 μm, even with electrode material sputtered on both sides, a flexible DBD setup could be achieved. While sputter-coating of dielectrics for plasma generation was used before on inflexible dielectrics [92, 93], and DBD configurations were built with flexible dielectrics [94–97] using metal tape as electrodes, thin films or printed circuit board technology, sputter-coating of electrode material on a flexible dielectric created a novel plasma source for medical applications.
Different electrode materials and electrode thicknesses were tested to prolong the lifespan of the plasma source. Here, the increase of resistance of the electrode material due to plasma generation was used as a marker for material changes and oxidation due to plasma treatment (compare with results of publication I). Another criterion was the minimal voltage needed to generate a homogeneous plasma ignition and electrode temperature during plasma ignition. From four different electrode materials, palladium (Pd) showed the best results and was hence used as electrode material for further experiments. The comparison of different electrode thicknesses (between 55 and 220 nm) showed the most stable and reliable homogeneous plasma ignition for values of 110 nm for both electrodes. Grounded electrode geometry was set to a spiral for maximal edge area and electrical connections were attached with plastic screws (compare section 2.3.2 and figure 2.7). As tested plasma parameters, three different configurations were chosen. Firstly, low ozone mode was defined as the lowest possible combination of input parameters (voltage and frequency) to generate a stable and homogeneous plasma ignition. Secondly, high ozone mode was chosen, where the combination of input parameters led to a pure and highly concentrated ozone generation. Thirdly, NO_X mode was set to the combination of input

parameters, which led to a pure nitrogen mode and hence only low ozone concentrations.
Again, bacteria deactivation properties of the air DBD plasma source prototype were proven for all three parameter configurations, this time by treatment of *E. coli* K12 MG1655 bacteria, and a characterization of the newly developed plasma source was made.
As a result, a 5.3 $\log_{10}$ reduction of cell forming units could be found within 5 minutes for lower input powers (high ozone mode), and for higher input powers (NO_X mode) a $\log_{10}$ reduction of 6.7 within 5 minutes could be achieved, while the detection limit was set to 7.7. D-values were less than 1 minute for all three setups. Power density was found to be 5-7 $\frac{mW}{cm^2}$ for ozone modes and between 25 and 33 $\frac{mW}{cm^2}$ for NO_X mode for the tested electrode thickness configurations of Pd. Erosion of electrodes, soldering joints and case material, which was an issue during CAP treatment with the SMD plasma chamber used during the first experimental series, was not found for the flexible sputter-coated DBD samples, neither for the 3D printed ASA material of the treatment box, but on the dielectric a border area along the grounded spiral electrode was found to develop. Despite these promising results, problems of burn through of the dielectric occurred for high input powers in NO_X mode. Life span of the NO_X mode CAP prototype could be prolonged by 150% to almost 150 minutes with cooling in between plasma treatments, but further improvements of this prototype are still necessary to reach longer total treatment times for NO_X mode. Additionally, active cooling with a fan during plasma treatment was tested, but ozone concentration measurements revealed, that the produced plasma changed from NO_X mode to transition mode. This corresponds to previous findings, where air flow through slits in the plasma source was found to destabilize plasma discharge [98]. However, prototypes that run in low and high ozone mode did not burn through during the whole experimental sequence and provided continuous and reliable results. With a total treatment time until the end of the experiments of 249 minutes ($\approx$ 4 hours) and a total number of 78 treatments, these two prototypes provided promising results during bacterial experiments (and are still working reliably) and hence, especially high ozone mode with an achieved bacteria $\log_{10}$ reduction of 5.3 could play a major role in developing a complete setup.
Comparing the bactericidal and sporicidal results of the two experimental series, a comparable $\log_{10}$ reduction is reached for both plasma sources. While $\log_{10}$ reduction was between 4.3 and 6.2 for ozone mode with the SMD setup in publication I, a $\log_{10}$ reduction of 5.3 was reached for high ozone mode of the novel air DBD plasma setup in publication II. While in publication I, $\log_{10}$ reductions were achieved within 15 minutes of plasma treatment, the $\log_{10}$ reduction mentioned above was achieved within 5 minutes of plasma treatment in publication II. One reason might be the smaller plasma treatment box volume of the setup used in publication II, another reason might be the difference in treated bacteria (*Bacillus atrophaeus* and *Escherichia coli*). Nevertheless shows the direct comparison of the disinfection properties of the two plasma sources the great potential of the tested prototype - with its input powers one order of magnitude smaller as the SMD plasma source's - and hence highlights the promising characteristics of the newly developed sputter-coated flexible DBD setup.

Chapter 4

Publication I: Surface modifications caused by cold atmospheric plasma sterilization treatment

List of contribution of each author to the article:

Sandra Moritz

- planning and conduction of experiments
- data acquisition
- data evaluation
- writing

Alisa Schmidt

- support and counsel for bacterial experiments
- proofreading

Joachim Sann

- data aquisition of XPS experiments
- proofreading

Markus H. Thoma

- proofreading
- provision of equipment

OPEN ACCESS
IOP Publishing
Journal of Physics D: Applied Physics
J. Phys. D: Appl. Phys. **53** (2020) 325203 (9pp)
https://doi.org/10.1088/1361-6463/ab88e9

Surface modifications caused by cold atmospheric plasma sterilization treatment

Sandra Moritz[1,3], **Alisa Schmidt**[1,3], **Joachim Sann**[2,3] **and Markus H Thoma**[1,3]

[1] Institute of Experimental Physics I, Justus Liebig University Giessen, Heinrich-Buff-Ring 16, 35392 Giessen, Germany
[2] Institute of Physical Chemistry, Justus Liebig University Giessen, Heinrich-Buff-Ring 17, 35392 Giessen, Germany
[3] Center for Materials Research (LaMa), Justus Liebig University Giessen, Heinrich-Buff-Ring 16, 35392 Giessen, Germany

E-mail: sandra.moritz@physik.uni-giessen.de

Received 12 February 2020, revised 28 March 2020
Accepted for publication 14 April 2020
Published 4 June 2020

Abstract

Inactivation of microorganisms on sensitive surfaces by cold atmospheric plasma is one major application in the field of plasma medicine because it provides a simple and effective way to sterilize heat-sensitive materials. Therefore, one has to know whether plasma treatment affects the treated surfaces, and thus causes long-term surface modifications. In this contribution, the effect of cold atmospheric Surface micro-discharge (SMD) plasma on different materials and its sporicidal behavior was investigated.

Hence, different material samples (stainless steel, different polymers and glass) were plasma-treated for 16 hours, simulating multiple plasma treatments using an SMD plasma device. Afterwards, the material samples were analyzed using surface analysis methods such as laser microscopy, contact angle measurements and x-ray photo-electron spectroscopy. Furthermore, the device was used to investigate the behavior of *Bacillus atrophaeus* endospores inoculated on material samples at different treatment times.

The interaction results for plasma-treated endospores show, that a log reduction of the spore count between 4.3 and 6.2 can be achieved within 15 min of plasma treatment. Besides, the surface analysis revealed, that there were three different types of reactions the probed materials showed to plasma treatment, ranging from no changes to shifts of the materials' free surface energies and oxidation.

As a consequence, it should be taken into account that even though cold atmospheric plasma treatment is a non-thermal method to inactivate microorganisms on heat-sensitive materials, it still affects surface properties of the treated materials. Therefore, the focus of future work must be a further classification of plasma-caused material modifications.

Keywords: cold atmospheric plasma, surface modification, plasma surface tratment, air dielectric barrier discharge, surface micro-discharge plasma, spore inactivation

(Some figures may appear in colour only in the online journal)

1. Introduction

The increase in bacterial resistances causes thousands of deaths every year due to a lack of quick and non-harming sterilization methods. Cold atmospheric plasma (CAP) treatment as a new approach to sterilize surfaces, particularly of heat-sensitive materials or difficult geometries (e.g. [1–5]), is a promising candidate to replace or support conventional cleaning methods.

Although in the last decade cold atmospheric plasma was increasingly used to inactivate bacteria, spores and fungi on different surface materials [6–8], e.g. hospital materials such as samples of marmoleum, mattress, polypropylene, powder-coated mild steel and stainless steel [9], or different polymers [10–13], the long-term influence of plasma treatment on these materials was rather neglected. Nevertheless, cold atmospheric plasma is composed of different highly reactive oxygen and nitrogen species (RONS) [14–18], e.g. O_3, H_2O_2, OH^-, HNO_3 and N_xO_y. Hence the reaction between plasma species and surface material has to be well-understood to be able to provide a safe and enduring surface cleaning method.

Recent studies observed etching effects during a dielectric barrier discharge (DBD) treatment [19], and oxidation effects of aluminum after 90 minutes treatment with surface micro-discharge (SMD) plasma [20]. Bartis *et al* [21] used 7 minute SMD treatment operated with N_2/O_2 mixtures to study functional groups of model polymers. Samples were analyzed directly after plasma treatment, and they found NO_3 groups attached to the surface. Surface analysis after treatment with atmospheric pressure plasma jet (APPJ) with different nitrogen and oxygen admixtures revealed material changes due to O_3 and NO_x [22, 23]. Knoll *et al* [10] investigated treatment with APPJ plasma at different distances from the plasma (direct contact vs. afterglow) and for the afterglow setup surface modifications of polymers were analyzed. Furthermore, the influence on polytetrafluorethylen (PTFE) and silicon was investigated by Shimizu *et al* [20]. Nevertheless, due to different setup geometries, plasma production methods, e.g. plasma jets (used for example by Walsh *et al*, Reuter *et al* and Knoll *et al* [10, 11, 24]), Floating-Electrode DBD (e.g. Fridman *et al* [25] or Kuzminova *et al* [19]) or SMD (e.g. used by Morfill *et al*, Klämpfl *et al* and Shimizu *et al* [20, 26, 27], and different carrier gases (e.g. argon, air and helium [3, 26, 28–31]), the interaction between plasma and target, as well as the gas composition and hence the plasma chemistry are affected in different ways [16], and therefore the results are not comparable [32]. Another point that should be taken into consideration is that usually only the effect of short plasma treatments with a time range of 30 s (Cahill *et al* [9]) to 90 minutes is investigated. Still, sterilization methods for clinical use are performed regularly, often several times per day.

Hence, in this study different material types, regularly used in hospitals, (stainless steel, polymers, glass) were treated with the same plasma source to obtain comparable results. Moreover, treatment time was extended up to 16 hours to investigate long-term effects and possible quality losses of the materials due to atmospheric plasma treatment and hence achieve clinical-relevant results. Subsequently, laser microscopy, contact angle measurements and XPS quantification were used to investigate surface modifications. Reuter *et al* [11] and Fauland *et al* [12] found an increase of hydrophility of polymers due to plasma treatment, but observed recovery processes within the following 120 h [11] and with increasing storage time [12], respectively. Homola *et al* [13] observed changes of polymer's surface energies due to plasma treatments and increased hydrophility with a stability of 3–5 days. To eliminate the measurement of short-term recovery mechanisms of the materials after plasma treatment, surface analysis was executed at least 4 weeks after the end of the long-term plasma treatment. As plasma setup, rather than using plasma jet or DBD technology, where the target is in direct contact with the plasma and the produced gas components, an SMD device was used as shown in figure 1(a). Thus, only long-living reactive species of the afterglow, that are more gentle to the material, could interact with the target [21, 26, 33, 34]. Additionally, the sporicidal properties of the plasma setup were verified probing *Bacillus atrophaeus* endospores on material samples of each group, and a possible connection between the extend of a material's surface modification and its sporicidal properties during plasma treatment was tested.

2. Materials and methods

2.1. SMD plasma system

A sketch of the used experimental setup is shown in figure 1(a). The SMD plasma system consists of a copper electrode driven at high voltage, quartz glass as dielectric and a grounded aluminum grid as counter electrode. An image of the generated plasma discharge is shown in figure 1(b), the discharge voltage and discharge current is displayed in figure 1(c). Within a distance of about 26 mm samples were placed on a grounded metal plate. In this experimental system, the plasma chamber is closed during the treatments by a movable cover, which is opened during the breaks to enable quick air exchange via natural convection in between plasma treatments.

Between grid and copper electrode, high voltage of 9 kV_{pp} at 2 kHz was applied using a high voltage amplifier (model 10/40A, Trek Inc.) with a sinusoidal signal, provided by the function generator (HM8150, Rohde & Schwarz). SMD plasma is then produced on the surface of the grid electrode. Power density $\left(\frac{P}{A}\right)$ at the SMD surface was measured to be 0.13 $\frac{W}{cm^2}$ using Lissajour's curve [35].

As material samples, stainless steel AISI 321 (S/S), rigid polyvinyl chloride (UPVC), polypropylene (PP), fluorinated ethylene propylene (FEP) (all GoodFellow) and borosilicate glass (Marienfeld) were chosen, for they are standard materials in the hygiene sector. Sporicidal efficacy of this SMD treatment on the chosen material samples was evaluated by placing the samples (cut to 10 mm × 10 mm; thickness of 0.914 mm (S/S) and 1 mm, respectively; glass samples with a diameter of 10 mm and thickness of 0.17 mm) inoculated with *Bacillus atrophaeus* endospores (Simicon) on the grounded metal plate of the plasma setup, and by treating them with afterglow plasma for different time spans, ranging from 5 to 15 minutes.

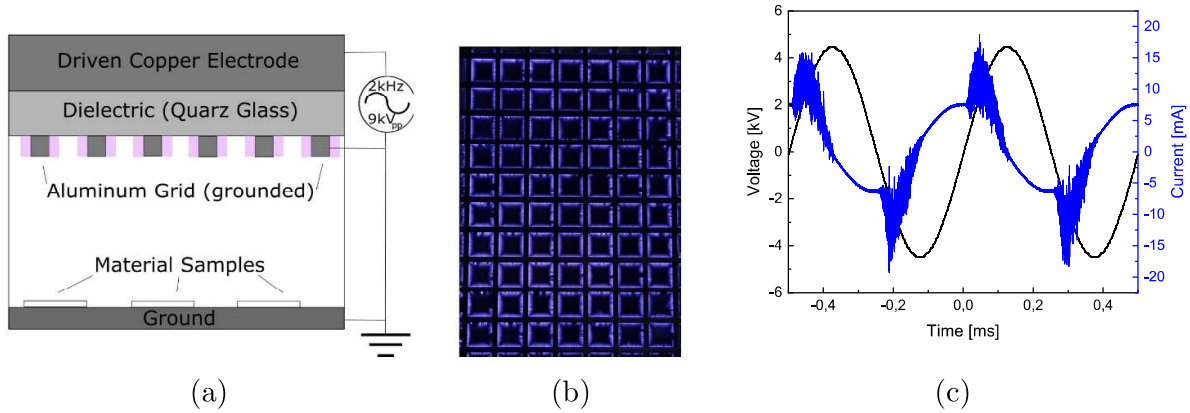

Figure 1. (a) SMD plasma setup and electric circuit. A copper electrode was connected to a voltage amplifier, quartz glass was used as dielectric, and a grounded aluminum grid served as counter electrode. Samples were placed at a distance of about 26 mm from the generated plasma on a grounded metal plate. (b) Image of plasma discharge and (c) discharge voltage and corresponding discharge current at 2 kHz and 9 kV_{PP}.

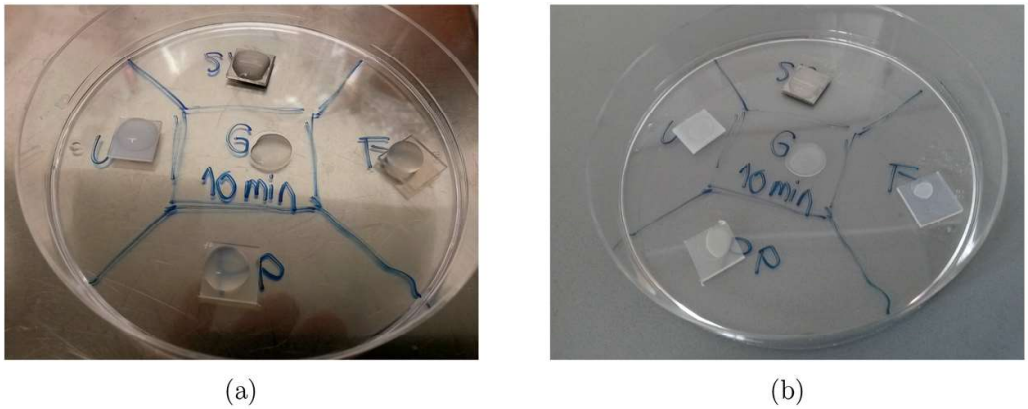

Figure 2. Material samples inoculated with master suspension of *Bacillus atrophaeus* endospores (left) and after overnight drying process (right).

For evaluating surface modifications caused by plasma treatment, the plasma chamber containing the samples was driven at room temperature for 16 hours (equivalent to about 190 5-minutes-treatments) with 10 minutes-breaks every 30 minutes. During breaks, the cover was opened to obtain a quick gas exchange with the surrounding air. During all treatments the relative humidity of the ambient environment was about 60–70%. Note, that S/S samples for surface analysis were mechanically polished first, to improve laser microscopy images.

Due to the distance between SMD plasma and sample, the produced plasma species were not instantly filling the whole plasma chamber. Ozone concentration, which was found to be strongly related to bacteria reduction [3, 36], was measured by absorption spectroscopy (HR4000CG-UV-NIR, Ocean Optics) using collimators, UV optical fibers and light from a UV deuterium lamp at a wavelength of 254 nm (D2000, Mikropack) within the SMD chamber's volume of 429 cm^3 at 22 mm distance from the plasma grid, to simulate the height of a sample in a petri dish. The light absorption was measured thrice for 30 minutes with 10 minutes of air exchange between plasma chamber and ambient air in between the measurements. The ozone concentration then was calculated using the Beer–Lambert law with an ozone absorption cross section of $1.1 \cdot 10^{-}21\ m^2$ [37].

2.2. Microbiological samples

Preparation of spore samples, plasma treatment and recovery of endospores were conducted analogously to the procedure in previous work [3] as listed below:

(a) As master suspension, *Bacillus atrophaeus* endospores in deionized water were used with a bacteria density of approximately $10^8\ ml^{-1}$.
(b) 100 μl (50 μl for glass samples due to smaller geometry) of this master suspension was subsequently spread on the material samples as shown in figure 2(a) and dried over night at the ambient air under the safety workbench (2(b)). Note that the shape of the dried drop differs between different materials, depending on their hydrophilic properties.
(c) The following day, the samples were placed in the plasma chamber as shown in figure 1(a).
(d) The samples were plasma-treated for 0 (reference samples), 5, 10, and 15 minutes, respectively.
(e) After plasma treatment, the samples were added to 2 ml of deionized water and vortexed for 1 min. This was followed by a 2 min ultrasonic treatment and another vortexing period of 1 min.

(f) To evaluate the number of surviving endospores, a dilution series was conducted. 100 μl of every degree of dilution was spread on agar plates. For 15 minutes treatment the 2 ml of the recovered spore suspension was spread completely on four agar plates with 500 μl on each.
(g) The agar plates were then incubated for up to 48 hours at 32 °C.
(h) After incubation the number of colony forming units (CFU) was counted to evaluate log reduction.

Experiments were performed at least thrice. After experiments, the samples were cleaned with ethanol and autoclaved for 15 minutes at 121 °C before reusing them.

For statistical analysis, diluted samples were only counted, if they had more than 3 CFU. Non-diluted samples with no CFU were counted as if one CFU in the 2 ml suspension was found. In figure 3(b) (results), data points, where at least once no CFU was found, are marked with a *.

For our experimental setup, the detection limit in log reduction of *Bacillus atrophaeus* endospores was between 6.2 and 6.8 for the different materials.

2.3. Surface analysis methods

The plasma-treated material samples (as described in the previous section) were tested for surface modifications using laser microscopy, contact angle measurements and XPS quantification. For preventing false results due to material changes caused by surface analysis methods, there was a set of material samples for each analysis method. Recovering effects of the materials, that may occur after plasma treatment, were excluded by performing surface analysis at least 4 weeks after plasma treatment. Reference samples, that were not plasma-treated, were tested at the same time as treated samples.

Firstly, for laser microscopy scanning the VK-9710 (Keyence) microscope, using 408 nm wavelength and 50x-fold magnification, provided a topographic scan of the surface, which was then examined using VK Analyzer (Keyence) to specify the roughness of the materials' surfaces. Three samples of each plasma-treated and non-treated material were investigated.

Secondly, contact angle measurements were executed using OCA 20 optical contact angle measuring and contour analysis system and SCA 20 and SCA 21 software (DataPhysics Instruments GmbH). As reference fluids, deionized water, ethanol, diiodomethane and ethylene glycol were used. The Sessile drop method [38] and, resulting from this data, calculation of the free surface energies of the sample materials were performed, evaluating also the polar and disperse fractions of the surface energy. The reference free surface energies for ethanol were taken from Ström *et al* [39], the others from Ohm *et al* [40] to calculate free surface energies of the material samples using OWRK-model [41–43]. For every material two plasma-treated samples and two reference samples were used and the experiments were executed twice on every sample.

Lastly, XP-spectroscopy was performed using VersaProbe II microscope (Physical Electronics GmbH) and CasaXPS software (Casa Software Ltd). The dual-beam charge neutralizer was driven using electrons with approximately 2 eV and argon ions (Ar^+) with 10 eV. During measurements, the surface potential was about 2 V due to higher electron flux (whereas the S/S samples were grounded due to their conductibility). Radiation source was a monochromatic Al-k α radiator with an energy of 1,486 eV. The x-ray power was about 90 W and the analysis area was 1.3 mm $\times$ 100 μm at high power mode. Transmitting energy of the analyzer was at 93.9 eV with a step size of 0.8 eV and an integration time of 50 ms. With the XPS microscope, one plasma-treated sample and one reference sample of every material were analyzed.

3. Results

In this paper, surface modifications caused by long-term SMD plasma treatment on S/S, glass, PP, UPVC and FEP were investigated in detail using laser microscopy, contact angle measurements and XPS-quantification. Moreover, sporicidal properties of the SMD plasma were verified, treating *Bacillus atrophaeus* endospores inoculated on the probed materials, and the ozone concentration in the plasma chamber was measured. As shown in figure 3(a), it takes approximately 5 min to reach a steady state ozone concentration.

Figure 3(b) shows the reduction of *Bacillus atrophaeus* endospores on different materials as a function of plasma treatment time at room temperature with a relative humidity of about 60–70%.

For S/S, a log reduction of 6.0 could be reached within 15 minutes of treatment time, for UPVC and glass log reduction was 6.2 and 5.6, respectively. For those materials spore reduction reaches close to the detection limits, whereas for FEP and PP a log reduction of 4.5 and 4.3, respectively, could be achieved. During the first 5 minutes, only a small bacteria reduction with a maximum of log 1 could be obtained. At a time period between 5 and 10 minutes, the reduction function became steep. Consequently, D-values were between 5 (S/S) and 6 minutes (FEP), while the reduction from log 1 to log 2 took only between 1 (glass) and 2 minutes (UPVC). After 10 minutes, log reduction became slower.

The surface analysis of the material samples showed a wide spectrum of modifications due to SMD treatment.

The surface roughness of treated materials stayed approximately the same (table 1), only for S/S, significant changes were observed, and a rusty-colored covering, also visible to the naked eye, was found after plasma-treatment (figure 4). Nevertheless, laser microscopy images of PP and UPVC showed a change of appearance (figure 5) whereas there were no visible changes for FEP samples (figure 6).

In accordance with the laser microscopy results, changes of the contact angle between probed samples and reference liquids (deionized water, ethanol, diiodomethane and ethylene glycol) for plasma-treated materials were detected (e.g. figure 7(a)). Again, FEP showed no detectable difference between plasma-treated and reference sample, in contrast to all other materials. Note, that only for S/S the contact angle got higher for the plasma-treated case, whereas glass, PP and

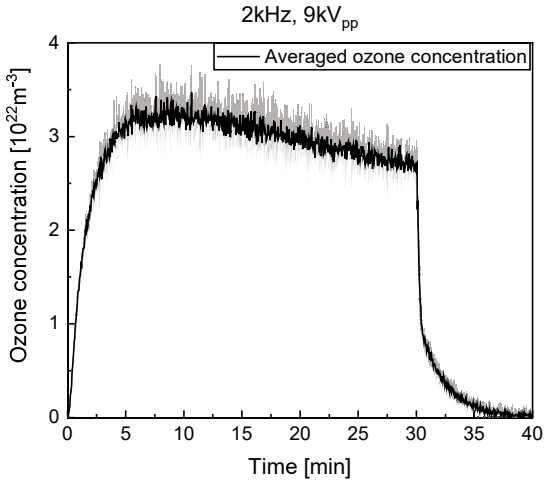

(a) Ozone concentration, derived with Beer-Lambert-Law, during 30 minutes of plasma treatment averaged over three treatment cycles with 10 minutes breaks with air circulation by natural convection between each cycle. The gray areas show the standard deviation.

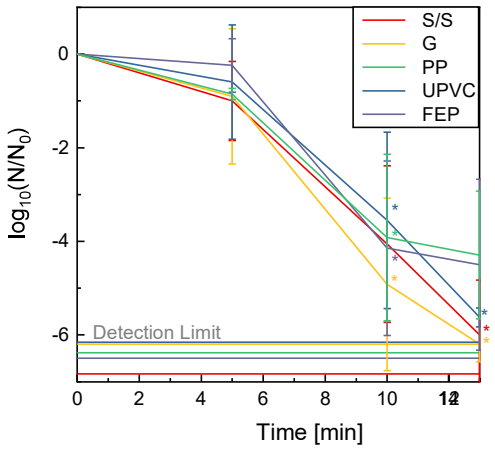

(b) Log reduction of *Bacillus atrophaeus* endospores at different treatment times. N is the number of CFU after plasma treatment, N_0 the number of CFU for the reference samples. Samples with no CFU were counted as explained in Materials&Methods.

Figure 3. Ozone concentration during plasma treatment time of 30 minutes and 10 minutes break afterwards (left) and log reduction curves of *Bacillus atrophaeus* endospores on different materials (right).

(a) S/S macroscopic; left is reference sample, right is plasma-treated

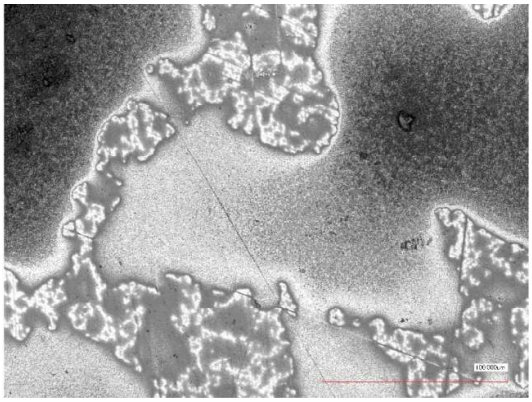

(b) Laser microscopic S/S image (plasma-treated)

Figure 4. After plasma-treatment, a brown, rusty cover appeared on the S/S samples. It was visible to the naked eye (a). More structures could be found with laser microscopy images (b).

Table 1. Roughness value R_a of different materials with and without plasma-treatment. Only S/S shows a significant change in surface roughness.

	plasma-treated	reference
S/S	0.111±0.084 μm	0.016±0.002 μm
Glass	–	–
PP	0.058±0.006 μm	0.056±0.011 μm
UPVC	0.018±0.003 μm	0.014±0.003 μm
FEP	0.037±0.006 μm	0.036±0.010 μm

UPVC became more hydrophilic (figure 7(a)). Using OWRK-modell, the samples' free surface energies with their disperse and polar fractions were calculated (figure 7(b)). S/S showed an increase of disperse fraction of free surface energy for plasma-treated case, while for glass, PP and UPVC the polar fraction increased. Besides, glass samples showed a significant

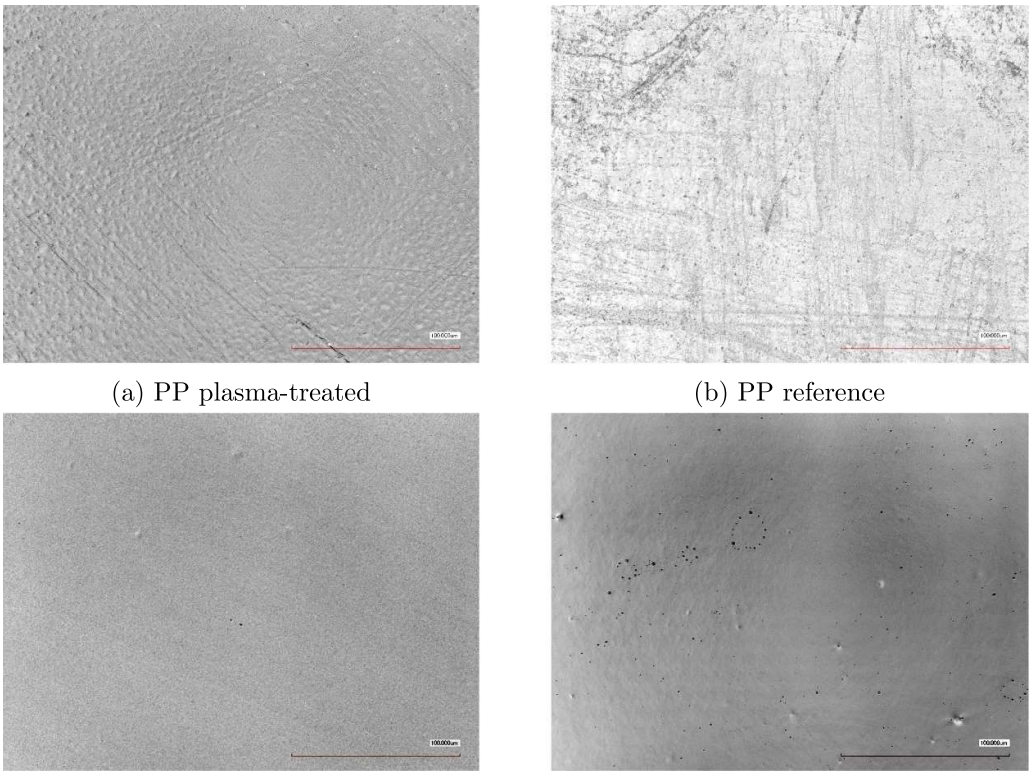

(a) PP plasma-treated (b) PP reference

(c) UPVC plasma-treated (d) UPVC reference

Figure 5. Laser microscopy identified a modification of the samples' surfaces. While the reference sample of PP (b) was rather flat and even, the plasma-treated sample (a) had a lot of dints at its surface. In contrast, plasma-treated UPVC samples (c) had a very planar morphology, while reference samples showed circular structures (d).

Table 2. Elemental composition of the material samples measured with XPS quantification with (left) and without (right) plasma treatment.

	plasma-treated (atomic-%)				reference (atomic-%)			
	O	C	N	Fe	O	C	N	Fe
S/S	54.1%	32.0%	7.5%	3.6%	36.4%	56.2%	1.3%	1.6%
Glass	67.0%	6.6%	0.8%		54.5%	15.5%	0.0%	
PP	10.8%	88.6%	0.6%		8.5%	90.2%	0.0%	
UPVC	10.7%	68.3%	0.7%		6.9%	78.1%	0.0%	
FEP	1.6%	37.9%	0.0%		1.2%	36.6%	0.0%	

increase of total free surface energy with a high increase of its polar fraction. In contrast, no significant changes between the plasma-treated and reference sample for FEP could be detected, yet there was a slight increase in the polar fraction and a slight decrease in the disperse fraction.

Finally, XPS analysis measured a quantified value for the surfaces' elemental composition. The results for plasma-treated FEP samples were again very similar to those of the reference samples (table 2). There was no nitrogen found and only small amounts of oxygen.

However, glass, PP and UPVC showed an increase of oxygen and nitrogen species on the surface. Although there was no nitrogen found for reference samples, there was roughly 0.5–1% found for plasma-treated samples.

Again, S/S showed the greatest change of elemental composition with an augmentation of the atomic concentration of oxygen, nitrogen and ferric on the surface. Note that oxygen and ferric concentration almost doubled while nitrogen concentration more than quintupled.

4. Discussion

After a long-term treatment of 16 h with atmospheric SMD plasma, three different material reactions can be found. As a first group, there is FEP, where no significant surface changes are found. Although there were minor changes in contact angle measurements and therefore in FEP's free surface energy, the measured values were so close to each other, that they laid within the error range. Hence, these changes are negligible. In the second group, slight changes in surface appearance and atomic concentration, accompanied with higher polar fractions of free surface energy were found. These effects were found for glass, as well as the polymers PP and UPVC.

As third group, there is S/S with significantly changed elemental composition, free surface energy properties and surface appearance.

Ozone concentration measurements revealed, that ozone is one of the main plasma products produced during the experiments, since its concentration reaches a steady-state range after 5 minutes of treatment time. The plasma settings therefore generate an SMD plasma in the so-called "ozone

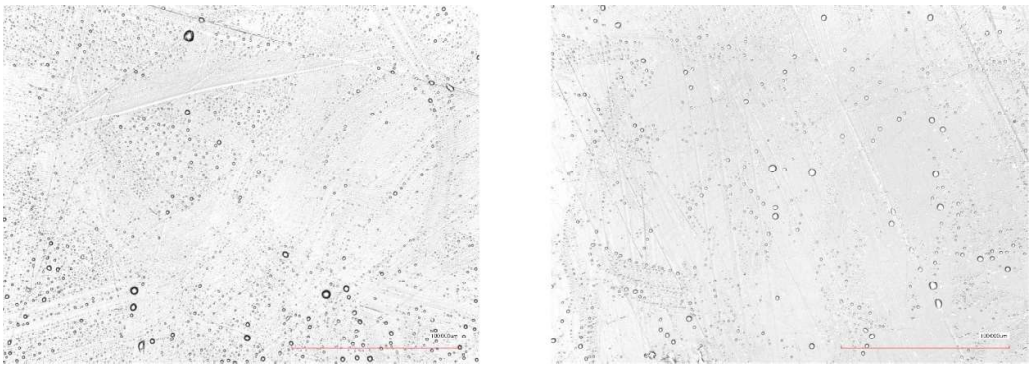

(a) FEP plasma-treated (b) FEP reference

Figure 6. FEP samples showed no modifications beetween plasma-treated (a) and reference sample (b) under laser microscopy.

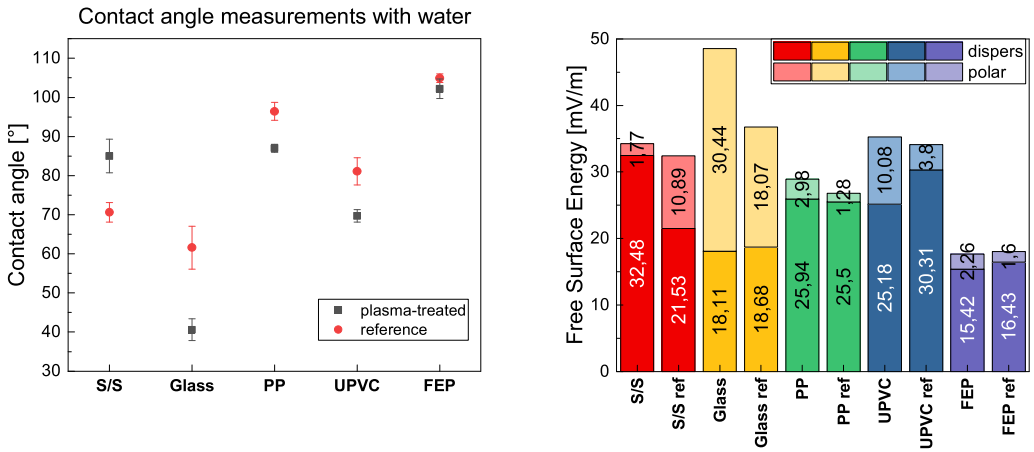

(a) (b)

Figure 7. Results of contact angle measurements of different materials with deionized water (a) and calculated polar and disperse fractions of free surface energies of the materials (b), respectively.

mode" [14, 44, 45]. Yet, nitrogen as major element in air also participates in plasma-surface interactions, as the XPS-measurements revealed. Hence, two different mechanisms explain the appearance of the rusty crust found on S/S samples, identified as ferrous oxide: firstly, nitrogen and oxygen interact as follows, producing nitric acid. Nitric acid oxidizes ferrous iron to ferrous oxide, with nitrogen dioxide and water as side products. Ferrous oxide and nitrogen dioxide react again with iron(III) oxide and nitrogen oxide as products:

$$\mathrm{N_2 + O_2 \rightarrow 2NO}$$
$$\mathrm{4NO + 3O_2 + 2H_2O \rightarrow 4HNO_3}$$
$$\mathrm{2HNO_3 + Fe \rightarrow 2NO_2 + H_2O + FeO}$$
$$\mathrm{2FeO + NO_2 \rightarrow Fe_2O_3 + NO.}$$

A second mechanism describes the reaction of ferrous iron and ozone:

$$\mathrm{2Fe + O_3 + 3H_2O \rightarrow 2Fe(OH)_3}$$
$$\mathrm{2Fe(OH)_3 \rightarrow Fe_2O_3 + 3H_{2O}.}$$

Note that in both reaction mechanisms water, which was accessible during the plasma treatment due to air humidity, served as a catalyst. The importance of high air humidity was also shown in [3]. The production of iron(III)oxide supports the findings of Shimizu *et al* [20], where aluminum was found to oxidize after exposure to CAP. The slight changes in surface appearance of PP and UPVC can be explained with etching mechanisms as they were found in [19], yet they were minor because of the weaker surface interaction of afterglow, that was used in this setup [34]. The increase in hydrophility for most materials is supported by the findings of Reuter *et al* [11] and Fauland *et al* [12], yet the changed hydrophility is still clearly detectable after 4 weeks between the last plasma treatment, while they observed decreases of hydrophility within 120 h [11]. Also the increase in free surface energy, that was found during the experiments of Homola *et al* [13] was very small for most samples. Only the fraction of polar and dispers free surface energies changed significantly.

Sporicidal experiments showed no parallels to the found surface modification groups because sporicidal effects were strongest for glass and S/S, followed by UPVC, and weakest for FEP and PP. Therefore, it is more likely, that differences in sporicidal effects are due to their different hydrophobic behavior and layering. If one compares the material's

contact angles with water (figure 7) and the images of sample preparation (figure 2(b)), it becomes obvious that the size of the area containing dried master solution in the experiments was smaller for PP and FEP because of their hydrophobic properties, whereas UPVC, glass and S/S were more hydrophilic, thus the same number of endospores were spread over a larger surface. As a consequence, layering phenomena, that shield the probed endospores partly, are more likely to influence the results for FEP and PP samples. In [3, 46], the link between layering mechanism and reduced bactericidal properties was also described.

5. Conclusion

After 16 hours of atmospheric SMD plasma treatment, three reaction groups of the different materials, S/S, UPVC, PP, FEP and glass, were found.

While the surface of FEP samples showed no reaction to plasma treatment, the other material's surfaces changed. These changes were found in XP spectroscopy (attachment of oxygen and nitrogen), contact angle measurements and free surface energies (change in hydrophobia, change of polar and disperse fractions of free surface energy), as well as in laser microscopy (slight changes of surface appearance for UPVC and PP and a higher surface roughness and a rusty crust for S/S). Especially for S/S, the ferrous iron in the alloy was found to react with reactive nitrogen and oxygen species and combine to iron(III) oxide. Consequently, the use of CAP in medical applications has to be considered carefully. The choice of material influences the plasma-surface reaction crucially, and advantages, e.g. low-temperature and difficult-geometry sterilization, and disadvantages, such as etching mechanisms of the surface and chemical reactions of treated materials with the surrounding air, even for rather weak afterglow plasma treatments, have to be taken into consideration. In future research, the change of surface properties due to long-term CAP treatment for more materials has to be done, especially for more polymers and different stainless steel alloys. Moreover, in future research more plasma parameters have to be investigated to find the optimal settings for a surface-preserving CAP treatment.

Sporicidal properties on the other hand were found to be only dependent on the materials' hydrophobic properties, and hence layering phenomena, but no correlation between the surfaces' sensitivity to CAP treatment and sporicidal effects was found. Nevertheless, the number of endospores on the sample's area, that is needed to prove sterilization properties, does not correlate with realistic cases, because rinsing and other cleaning methods reduce the number of microorganisms before sterilization treatment, and microorganisms are usually spread over a larger surface. In future work the aim will be to use a larger surface area with multiple droplets with lower concentrations spread over it to achieve higher spore surface density exposed to plasma.

The aim of this study was the identification of possible surface modifications of different materials due to long-term sporicidal cold atmospheric plasma treatment. Changes in appearance, free surface energy and surface elemental composition were found after 16 hours of plasma treatment for most materials, while bactericidal effects of the experimental setup were proven.

Acknowledgments

S Moritz wants to thank her collaborators Janosch J Perlbach and Markus Göttlicher for their support in the laboratory.

ORCID iD

Sandra Moritz https://orcid.org/0000-0003-1363-403X

References

[1] Critzer F J, Kelly-Wintenberg K, South S L and Golden D A 2007 Atmospheric plasma inactivation of foodborne pathogens on fresh produce surfaces *J. Food Protect.* **70** 2290–6

[2] Stoffels E, Sakiyama Y and Graves D B 2008 Cold atmospheric plasma: charged species and their interactions with cells and tissues *IEEE Trans. Plasma Sci.* **36** 1441–57

[3] Mandler J, Moritz S, Binder S, Shimizu T, Müller M, Thoma M and Zimmermann J L 2017 Disinfection of dental equipment—inactivation of Enterococcus mundtii on stainless steel and dental handpieces using surface micro-discharge plasma *Plasma Med.* **7** 407–16

[4] Arora V, Nikhil V, Suri N and Arora P 2014 Cold atmospheric plasma (CAP) in dentistry *Dentistry* **4** 1

[5] Jiang C, Chen M, Schaudinn C, Gorur A, Vernier P T, Costerton J W, Jaramillo D E, Sedghizadeh P P and Gundersen M A 2009 Pulsed atmospheric-pressure cold plasma for endodontic disinfection *IEEE Trans. Plasma Sci.* **37** 1190–5

[6] Lee K, Paek K, Ju W T and Lee Y 2006 Sterilization of bacteria, yeast and bacterial endospores by atmospheric-pressure cold plasma using helium and oxygen *J. Microbiol.* **44** 269–75

[7] Klämpfl T G, Isbary G, Shimizu T, Li Y F, Zimmermann J L, Stolz W, Schlegel J, Morfill G E and Schmidt H-U 2012 Cold atmospheric air plasma sterilization against spores and other microorganisms of clinical interest *Appl. Environ. Microbiol.* **78** 5077–82

[8] Nguyen L, Lu P, Boehm D, Bourke P, Gilmore B F, Hickok N J and Freeman T A 2018 Cold atmospheric plasma is a viable solution for treating orthopedic infection: a review *Biological chemistry* **400** 77–86

[9] Cahill O, Claro T, O'Connor N, Cafolla A, Stevens N, Daniels S and Humphries H 2014 Cold air plasma to decontaminate inanimate surfaces of the hospital environment *Appl. Environ. Microbiol.* **80** 2004

[10] Knoll A J, Luan P, Bartis E A J, Hart C, Raitses Y and Oehrlein G S 2014 Real time characterization of polymer surface modifications by an atmospheric-pressure plasma jet: Electrically coupled versus remote mode *Appl. Phys. Lett.* **105** 171601

[11] Reuter S, Niemi K, Gathen V and Döbele H 2007 The atmospheric pressure plasma jet as an atomic oxygen source for polymer treatment Treatment *3rd Int. Workshop Cold Atmospheric Pressure Plasmas: Sources and Applications*

[12] Fauland G, Constantin F, Gaffar H and Bechtold T 2015 Production scale plasma modification of polypropylene baselayer for improved water management properties *J. Appl. Polym. Sci.* **132** 41294

[13] Homola T, Matoušek J, Hergelová B, Kormunda M, Wu L Y and Černák M 2012 Activation of poly (methyl methacrylate) surfaces by atmospheric pressure plasma *Polym. Degrad. Stab.* **97** 886–92
[14] Tschang C Y T and Thoma M 2019 In vitro comparison of direct plasma treatment and plasma activated water on escherichia coli using a surface micro-discharge *J. Phys. D: Appl. Phys.* **53** 055201
[15] Kim S J and Chung T 2016 Cold atmospheric plasma jet-generated RONS and their selective effects on normal and carcinoma cells *Sci. Rep.* **6** 20332
[16] Pavlovich M J, Clark D S and Graves D B 2014 Quantification of air plasma chemistry for surface disinfection *Plasma Sources Sci. Technol.* **23** 065036
[17] Tschang C Y T, Bergert R, Mitic S and Thoma M 2020 Effect of external axial magnetic field on a helium atmospheric pressure plasma jet and plasma-treated water *J. Phys. D: Appl. Phys.* **53** 215202
[18] Ka upe J, Tschang C Y T, Birk F, Coenen D, Thoma M H and Mitic S 2019 Effect of cold atmospheric plasmas on bacteria in liquid: The role of gas composition *Plasma Process. Polym.* **16** 1800196
[19] Kuzminova A, Kretková T, Kylián O, Hanuš J, Khalakhan I, Prukner V, Doležalová E, Šimek M and Biederman H 2017 Etching of polymers, proteins and bacterial spores by atmospheric pressure DBD plasma in air *J. Phys. D: Appl. Phys.* **50** 135201
[20] Shimizu S *et al* 2014 Cold atmospheric plasma–a new technology for spacecraft component decontamination *Planet. Space Sci.* **90** 60–71
[21] Bartis E A, Luan P, Knoll A J, Graves D B, Seog J and Oehrlein G S 2016 A comparative study of biomolecule and polymer surface modifications by a surface microdischarge *Eur. Phys. J.* D **70** 1–19
[22] Bartis E A J, Graves D B, Seog J and Oehrlein G S 2013 Atmospheric pressure plasma treatment of lipopolysaccharide in a controlled environment *J. Phys. D: Appl. Phys.* **46** 312002
[23] Bartis E A J, Luan P, Knoll A J, Hart C, Seog J and Oehrlein G S 2015 Polystyrene as a model system to probe the impact of ambient gas chemistry on polymer surface modifications using remote atmospheric pressure plasma under well-controlled conditions *Biointerphases* **10** 029512
[24] Walsh J L, Shi J and Kong M G 2006 Contrasting characteristics of pulsed and sinusoidal cold atmospheric plasma jets *Appl. Phys. Lett.* **88** 171501
[25] Fridman G, Shereshevsky A, Jost M M, Brooks A D, Fridman A, Gutsol A, Vasilets V and Friedman G 2007 Floating electrode dielectric barrier discharge plasma in air promoting apoptotic behavior in melanoma skin cancer cell lines *Plasma Chem. Plasma Process.* **27** 163–76
[26] Morfill G, Kong M G and Zimmermann J 2009 Focus on plasma medicine *New J. Phys.* **11** 115011
[27] Maisch T, Shimizu T, Isbary G, Heinlin J, Karrer S, Klämpfl T, Li Y-F, Morfill G and Zimmermann J L 2012 Contact-free inactivation of *Candida albicans* biofilms by cold atmospheric air plasma *Appl. Environ. Microbiol.* **78** 4242–7
[28] Schmidt-Bleker A, Winter J, Bösel A, Reuter S and Weltmann K D 2015 On the plasma chemistry of a cold atmospheric argon plasma jet with shielding gas device *Plasma Sources Sci. Technol.* **25** 015005
[29] Ly L *et al* 2018 A new cold plasma jet: performance evaluation of cold plasma, hybrid plasma and argon plasma coagulation *Plasma* **1** 189–200
[30] Darny T, Pouvesle J M, Fontane J, Joly L, Dozias S and Robert E 2017 Plasma action on helium flow in cold atmospheric pressure plasma jet experiments *Plasma Sources Sci. Technol.* **26** 105001
[31] Lin L, Lyu Y, Trink B, Canady J and Keidar M 2019 Cold atmospheric helium plasma jet in humid air environment *J. Appl. Phys.* **125** 153301
[32] Jablonowski H, Sousa J, Weltmann K D, Wende K and Reuter S 2018 Quantification of the ozone and singlet delta oxygen produced in gas and liquid phases by a non-thermal atmospheric plasma with relevance for medical treatment *Sci. Rep.* **12** 8
[33] Mok C, Lee T and Puligundla P 2015 Afterglow corona discharge air plasma (ACDAP) for inactivation of common food-borne pathogens *Food Res. Int.* **69** 418–23
[34] Moreau S, Moisan M, Tabrizian M, Barbeau J, Pelletier J, Ricard A and Yahia L'H 2000 Using the flowing afterglow of a plasma to inactivate Bacillus subtilis spores: Influence of the operating conditions *J. Appl. Phys.* **88** 1166–74
[35] Hoł ub M 2012 On the measurement of plasma power in atmospheric pressure DBD plasma reactors *Int. J. Appl. Electromagn. Mech.* **39** 81–7
[36] Sakiyama Y, Graves D B, Chang H W, Shimizu T and Morfill G E 2012 Plasma chemistry model of surface microdischarge in humid air and dynamics of reactive neutral species *J. Phys. D: Appl. Phys.* **45** 425201
[37] Bass A and Paur R 1985 The ultraviolet cross-sections of ozone: I. The measurements *Atmospheric Ozone* Springer pp 606–10
[38] Staicopolus D 1962 The computation of surface tension and of contact angle by the sessile-drop method *J. Colloid Sci.* **17** 439–47
[39] Ström G, Fredriksson M and Stenius P 1987 Contact angles, work of adhesion and interfacial tensions at a dissolving hydrocarbon surface *J. Colloid Interface Sci.* **119** 352–61
[40] Ohm A and Lippold B 1986 Charakterisierung der benetzbarkeit von arzneistoffpulvern mit Hilfe der sessile drop-technik II: kritische oberflächenspannung und randwinkel/oberflächenspannungs-kurven *Pharmazeutische Indus.* **48** 508–13
[41] Owens D K and Wendt R 1969 Estimation of the surface free energy of polymers *J. Appl. Polym.* **13** 1741–7
[42] Rabel W 1971 Einige Aspekte der Benetzungstheorie und ihre Anwendung auf die Untersuchung und Veränderung der Oberflächeneigenschaften von Polymeren *Farbe Lack* **77** 997–1005
[43] Kaelble D 1970 Dispersion-polar surface tension properties of organic solids *J. Adhesion* **2** 66–81
[44] Pavlovich M J, Chang H W, Sakiyama Y, Clark D S and Graves D B 2013 Ozone correlates with antibacterial effects from indirect air dielectric barrier discharge treatment of water *J. Phys. D: Appl. Phys.* **46** 145202
[45] Shimizu T, Sakiyama Y, Graves D B, Zimmermann J L and Morfill G E 2012 The dynamics of ozone generation and mode transition in air surface micro-discharge plasma at atmospheric pressure *New J. Phys.* **14** 103028
[46] Yu H, Perni S, Shi J J, Wang D Z, Kong M G and Shama G 2006 Effects of cell surface loading and phase of growth in cold atmospheric gas plasma inactivation of Escherichia coli K12 *J. Appl. Microbiol.* **101** 1323–30

Chapter 5

Publication II: Characterization of Sputter-Coated Polyethylene Naphthalate-Foil as Novel Flexible Surface DBD Plasma Source

List of contribution of each author to the article:

Sandra Moritz

- design of electrode geometry
- design of experimental setup
- planning and conduction of experiments
- data acquisition
- data evaluation
- writing

Roman Bergert

- recommendation of PEN-material
- recommendation of circuit assembling
- proofreading

Martin Becker

- sputter-coating of materials
- advice on coating variables
- writing of section II A 1
- proofreading

Markus H. Thoma

- proofreading
- provision of equipment

Plasma Medicine, 13(2):27–46 (2023)

Characterization of Sputter-Coated Polyethylene Naphthalate-Foil as Novel Flexible Surface DBD Plasma Source

Sandra Moritz,[a,*] Roman Bergert,[b] Martin Becker,[a] & Markus H. Thoma[a]

[a]Justus Liebig University, I. Physical Institute, 35392 Gießen, Germany; [b]Justus Liebig University, II. Physical Institute, 35392 Gießen, Germany

*Address all correspondence to: Sandra Moritz, Justus Liebig University, I. Physical Institute, 35392 Gießen, Germany, E-mail: sandra.moritz@physik.uni-giessen.de

ABSTRACT: Plasma medicine demands for very specific plasma source configurations. Beside gas-flow-driven jet arrays, dielectrical barrier discharges (DBDs) are commonly used to generate ambient air plasma at room temperature for decontamination. There, electrode and dielectric material limit its use in application. Especially, the decontamination of difficult, uneven, or edged surface geometries with DBDs can be rather challenging. Therefore, flexible polyethylene naphthalate-foil with a thickness of 250 μm, which was covered with electrode material by ion-beam sputtering, is characterized regarding its electrical and bactericidal performance for different power and electrode thickness configurations. Operating temperature, ozone production capability, and plasma parameters (electron temperature and density as well as vibrational temperature of N_2) were used as characterization parameters. As electrode material, palladium sputtered with a thickness of 110 nm showed the best results of the tested materials. With operation parameters of 3 kHz and 5.5–6.0 kV_{pp} for ozone and 5 kHz and 8.5 kV_{pp} for nitrogen mode log reductions of up to 6.7 (nitrogen mode) and 5.3 (ozone mode), respectively, and D values of 1 min were accomplished for *Escherichia coli*.

KEY WORDS: CAP, cold plasma, SMD, flexible DBD, PEN, sputtering, surface DBD

0278–940X/23/$35.00

Chapter 6

Conclusion and Perspective

The aim of this thesis was the construction and characterization of a cold atmospheric plasma source for clinical application. During several experiments, the long-term influence of cold atmospheric plasma afterglow treatment on different materials, and hence their suitability for plasma decontamination and as material for plasma source setups was tested. Afterwards, a novel CAP source was constructed and its construction parts were tested for their eligibility in the context of plasma medicine. Here, PEN foil was tested as novel dielectric in ozone and nitrogen mode, because of its promising dielectric strength and excellent chemical resistance. In addition, the functionality of flexible electrodes, produced by sputter-coating was verified, and different electrode materials were tested for their plasma resistance. Besides, bactericidal and sporicidal effects of cold atmospheric plasma treatment with the studied and the newly developed plasma source were shown to validate the use of these devices for decontamination in a clinical environment.

Surface modification studies, focusing for the first time on the long-term effects of cold plasma afterglow treatment, showed a general change of wettability, change of polar and disperse fractions of free surface energy, attachment of oxygen and nitrogen species to the surfaces and changes of surface morphology. While stainless steel in particular showed strong surface modifications caused by surface oxidation, the polymer and glass samples showed significantly lower modifications. One polymer-sample, FEP, showed almost no surface modification at all.
During sporicidal experiments, a $\log_{10}$ reduction in spore count of 4.3-6.2 within 15 minutes could be achieved, depending on the material. Differences in reduction effectiveness seemed to be caused by the hydrophobic properties of the material, and hence stacking and shielding mechanisms, rather than by plasma-caused surface modifications of the materials. Plasma parameters were set to an ozone mode configuration and a power density of 130 $\frac{mW}{cm^2}$ was achieved.
This leads to the assumption, that a regular decontamination with CAP is appropriate for different materials, especially glasses and polymers, while metals seem to be more prone to modifications caused by CAP treatment. Given that standard decontamination treatments influence the decontaminated surface material as well [27, 28, 99–102], CAP treatment might be an alternative decontamination treatment for materials, where standard decontamination methods are limited, e.g. due to heat-sensitive characteristics of the material. Additionally, the changes of composition of the surface free energy could be seen as a beneficial side effect of plasma treatment for specific applications. Furthermore, given the fact that polymer is only the generic term of a wide range of materials, the research of plasma-polymer interaction opens up new possibilities for CAP source assembling.

As a consequence, in a second experimental series, PEN - a polymer with excellent

chemical resistance and a high dielectric strength - was tested as dielectric. Moreover, ion-beam sputtering was tested as production mechanism of flexible CAP-sources, by sputter-coating the electrode material directly onto the dielectric, and different electrode materials and electrode thicknesses were tested for their suitability as plasma source electrode. Thereby, a flexible CAP-source prototype was built and characterized. For characterization, plasma diagnostic parameters in NO_X mode were calculated, and plasma power density, grounded electrode temperature and plasma treatment temperature were evaluated. During characterization, ozone production was monitored, to evaluate plasma parameter for ozone and NO_X mode. Moreover, the bactericidal efficacy of the newly developed plasma source was proven and classified for NO_X, high ozone and low ozone mode. Here, the differentiation between high and low ozone mode was taken, to define the bactericidal efficacy for the lowest possible input power where a homogeneous and stable plasma ignition could be generated, and for the highest possible plasma parameters in pure ozone mode, just before transition mode. For NO_X mode plasma parameters were found, where the measured ozone curve overcame transition mode. Thus, a range of plasma parameters could be found, where plasma operation in pure ozone mode, as well as in pure NO_X mode, was possible for the newly developed plasma source. During experiments, bactericidal efficacy showed to be highest for NO_X mode, with a $\log_{10}$ reduction of 6.7 within 5 minutes, but at the same time NO_X mode showed a shorter life span of the CAP source prototype, as it burned through after 50 plasma operations (corresponding to $\approx$ 150 minutes). High and low ozone mode CAP source prototypes were, at the end of the experimental tests, still working reliably, with a total treatment time of thus far 249 minutes, corresponding to 78 plasma operations. While electrodes and electrical connections of the CAP source used during the first experimental series (see chapter 4) eroded and had to be cleaned and renewed regularly, the novel flexible CAP source with sputter-coated electrodes showed no erosion in ozone mode during the experiments and shows, as a consequence, a clear improvement to the SMD plasma source used before. High ozone mode showed high bactericidal efficacy as well, with an achieved bacterial $\log_{10}$ reduction of 5.3 within 5 minutes for bacteria solution concentrations of 10^8/ml. Here again, stacking and shielding mechanisms seemed to be a limiting factor in log reduction. Nevertheless, D-values were less than one minute for all tested plasma modes. Compared to the results of the first experimental series, decontamination efficacy of both plasma sources showed to be similar. At the same time, power densities of the novel plasma source both for ozone and NO_X modes were with values between 5 and 33 $\frac{mW}{cm^2}$ at least one order of magnitude smaller and hence, the novel plasma source showed an improvement in effectiveness, compared with the SMD plasma source.

To summarize the results, repetitive plasma treatment of different materials, over a long period of time, indicated CAP treatment as a successful and non-destructive cleaning-method for a wide range of materials, where material modifications stayed on an acceptable level. PEN, as newly characterized dielectric for DBD plasma sources, showed promising results to realize flexible, geometry-adaptable and save decontamination. As stacking during bacteria sample preparation was found to be a limiting factor of bacteria decontamination, cold atmospheric plasma could play a major role in enhancing log reduction of conventional sterilization methods by adding a plasma treatment after the conventional sterilization.
Yet, experiments to determine the plasma source's life span in ozone mode, and to extend the plasma source's life span in NO_X mode have to be conducted, e.g. by

embedding the DBD device into a cooling chamber or probing electrode thicknesses between 110 and 220 nm for their durability. Moreover, more dielectric and electrode materials should be tested for their suitability as flexible DBD source.
Combining the results, cold atmospheric plasma decontamination should be used, at least in addition to conventional sterilization methods, to improve pathogen reduction and obtain higher log reductions for the decontamination and sterilization of materials - especially heat sensitive or geometry complex - where traditional methods fall short, or are difficult and expensive to realize, as for space application.

Bibliography

1. Murray, C. J. *et al.* Global burden of bacterial antimicrobial resistance in 2019: a systematic analysis. *The lancet* **399,** 629–655 (2022).
2. Cassini, A. *et al.* Attributable deaths and disability-adjusted life-years caused by infections with antibiotic-resistant bacteria in the EU and the European Economic Area in 2015: a population-level modelling analysis. *The Lancet infectious diseases* **19,** 56–66 (2019).
3. Agyeman, W. Y. *et al.* A systematic review of antibiotic resistance trends and treatment options for hospital-acquired multidrug-resistant infections. *Cureus* **14** (2022).
4. Fridman, G. *et al.* Applied plasma medicine. *Plasma processes and polymers* **5,** 503–533 (2008).
5. Kong, M. G. *et al.* Plasma medicine: an introductory review. *New Journal of Physics* **11,** 115012. https://dx.doi.org/10.1088/1367-2630/11/11/115012 (2009).
6. Oliveira, A. C. D. d. *et al.* Application of cold atmospheric plasma for decontamination of toxigenic fungi and mycotoxins: A systematic review. *Frontiers in Microbiology* **15,** 1502915 (2025).
7. Jenns, K. *et al.* Inactivation of foodborne viruses: Opportunities for cold atmospheric plasma. *Trends in Food Science & Technology* **124,** 323–333 (2022).
8. Bunz, O. *et al.* Cold atmospheric plasma as antiviral therapy–effect on human herpes simplex virus type 1. *Journal of General Virology* **101,** 208–215 (2020).
9. Otto, C. *et al.* Physical methods for cleaning and disinfection of surfaces. *Food Engineering Reviews* **3,** 171–188 (2011).
10. Katsigiannis, A. S., Bayliss, D. L. & Walsh, J. L. Cold plasma for the disinfection of industrial food-contact surfaces: An overview of current status and opportunities. *Comprehensive Reviews in Food Science and Food Safety* **21,** 1086–1124 (2022).
11. Busco, G., Robert, E., Chettouh-Hammas, N., Pouvesle, J.-M. & Grillon, C. The emerging potential of cold atmospheric plasma in skin biology. *Free Radical Biology and Medicine* **161,** 290–304. ISSN: 0891-5849. https://www.sciencedirect.com/science/article/pii/S0891584920312776 (2020).
12. Daeschlein, G. *et al.* Skin and wound decontamination of multidrug-resistant bacteria by cold atmospheric plasma coagulation. *JDDG: Journal der Deutschen Dermatologischen Gesellschaft* **13,** 143–149 (2015).
13. Isbary, G. *et al.* A first prospective randomized controlled trial to decrease bacterial load using cold atmospheric argon plasma on chronic wounds in patients. *British Journal of Dermatology* **163,** 78–82. ISSN: 0007-0963. eprint: https://academic.oup.com/bjd/article-pdf/163/1/78/47499587/bjd0078.pdf. https://doi.org/10.1111/j.1365-2133.2010.09744.x (July 2010).

14. Ratovitski, E. A. *et al.* Anti-cancer therapies of 21st century: novel approach to treat human cancers using cold atmospheric plasma. *Plasma Processes and Polymers* **11,** 1128–1137 (2014).
15. Limanowski, R., Yan, D., Li, L. & Keidar, M. Preclinical Cold Atmospheric Plasma Cancer Treatment. *Cancers* **14.** ISSN: 2072-6694. https://www.mdpi.com/2072-6694/14/14/3461 (2022).
16. Yan, D. *et al.* Cold Atmospheric Plasma Cancer Treatment, a Critical Review. *Applied Sciences* **11.** ISSN: 2076-3417. https://www.mdpi.com/2076-3417/11/16/7757 (2021).
17. Han, X., Kapaldo, J., Liu, Y., Stack, M. S. & Ptasinska, S. Cold Atmospheric Plasma as a Novel Tool for Cancer Treatment. *Bulletin of the American Physical Society* (2015).
18. Maisch, T. *et al.* Contact-free inactivation of Candida albicans biofilms by cold atmospheric air plasma. *Applied and environmental microbiology* **78,** 4242–4247 (2012).
19. Kamionka, J. *et al.* Efficiency of cold atmospheric plasma, cleaning powders and their combination for biofilm removal on two different titanium implant surfaces. *Clinical Oral Investigations,* 1–9 (2022).
20. Klämpfl, T. G. *et al.* Cold atmospheric air plasma sterilization against spores and other microorganisms of clinical interest. *Applied and environmental microbiology* **78,** 5077–5082 (2012).
21. Hoon Park, J. *et al.* A comparative study for the inactivation of multidrug resistance bacteria using dielectric barrier discharge and nano-second pulsed plasma. *Scientific reports* **5,** 13849 (2015).
22. Nasir, N. M., Lee, B., Yap, S. S., Thong, K. & Yap, S. L. Cold plasma inactivation of chronic wound bacteria. *Archives of biochemistry and biophysics* **605,** 76–85 (2016).
23. Zimmermann, J. *et al.* Test for bacterial resistance build-up against plasma treatment. *New Journal of Physics* **14,** 073037 (2012).
24. Bruggeman, P. J. *et al.* Plasma–liquid interactions: a review and roadmap. *Plasma Sources Science and Technology* **25,** 053002. https://dx.doi.org/10.1088/0963-0252/25/5/053002 (2016).
25. Song, C.-H. *et al.* Cocktail of reactive species generated by cold atmospheric plasma: oral administration induces non-small cell lung cancer cell death. *Journal of Physics D: Applied Physics* **54,** 185202 (2021).
26. Bárdos, L. & Baránková, H. Cold atmospheric plasma: Sources, processes, and applications. *Thin Solid Films* **518,** 6705–6713. ISSN: 0040-6090. https://www.sciencedirect.com/science/article/pii/S0040609010009946 (2010).
27. Grinshpun, S. A., Yermakov, M. & Khodoun, M. Autoclave sterilization and ethanol treatment of re-used surgical masks and N95 respirators during COVID-19: impact on their performance and integrity. *Journal of Hospital Infection* **105,** 608–614 (2020).
28. Zhao, L. *et al.* The role of sterilization in the cytocompatibility of titania nanotubes. *Biomaterials* **31,** 2055–2063. ISSN: 0142-9612. https://www.sciencedirect.com/science/article/pii/S0142961209013477 (2010).
29. Pankaj, S. K. *et al.* Applications of cold plasma technology in food packaging. *Trends in Food Science & Technology* **35,** 5–17 (2014).

30. Mandler, J. *et al.* Disinfection of dental equipment—inactivation of Enterococcus mundtii on stainless steel and dental handpieces using surface microdischarge plasma. *Plasma Medicine* **7** (2017).
31. Müller, M. *et al.* Plasma afterglow circulation apparatus for decontamination of spacecraft equipment. *AIP Advances* **8** (2018).
32. May, G. S., Huang, J. & Spanos, C. J. Statistical experimental design in plasma etch modeling. *IEEE Transactions on Semiconductor Manufacturing* **4,** 83–98 (1991).
33. Al-Abduly, A., Christensen, P. & Harvey, A. The characterization of a packed bed plasma reactor for ozone generation. *Plasma Sources Science and Technology* **29,** 035002 (2020).
34. Martusevich, A. K. *et al.* Cold Argon Athmospheric Plasma for Biomedicine: Biological Effects, Applications and Possibilities. *Antioxidants* **11.** ISSN: 2076-3921. `https://www.mdpi.com/2076-3921/11/7/1262` (2022).
35. Bartis, E., Graves, D., Seog, J & Oehrlein, G. Atmospheric pressure plasma treatment of lipopolysaccharide in a controlled environment. *Journal of Physics D: Applied Physics* **46,** 312002 (2013).
36. Bartis, E. A. *et al.* Polystyrene as a model system to probe the impact of ambient gas chemistry on polymer surface modifications using remote atmospheric pressure plasma under well-controlled conditions. *Biointerphases* **10** (2015).
37. Bartis, E. A. *et al.* A comparative study of biomolecule and polymer surface modifications by a surface microdischarge. *The European Physical Journal D* **70,** 1–19 (2016).
38. Kuzminova, A *et al.* Etching of polymers, proteins and bacterial spores by atmospheric pressure DBD plasma in air. *Journal of Physics D: Applied Physics* **50,** 135201 (2017).
39. Shimizu, S. *et al.* Cold atmospheric plasma–A new technology for spacecraft component decontamination. *Planetary and space science* **90,** 60–71 (2014).
40. Fauland, G., Constantin, F., Gaffar, H. & Bechtold, T. Production scale plasma modification of polypropylene baselayer for improved water management properties. *Journal of Applied Polymer Science* **132** (2015).
41. Homola, T. *et al.* Activation of poly (methyl methacrylate) surfaces by atmospheric pressure plasma. *Polymer degradation and stability* **97,** 886–892 (2012).
42. Lu, X., Reuter, S., Laroussi, M. & Liu, D. *Nonequilibrium atmospheric pressure plasma jets: Fundamentals, diagnostics, and medical applications* (CRC Press, 2019).
43. Moritz, S., Schmidt, A., Sann, J. & Thoma, M. H. Surface modifications caused by cold atmospheric plasma sterilization treatment. *Journal of Physics D: Applied Physics* **53,** 325203 (2020).
44. Moritz, S., Bergert, R., Becker, M. & Thoma, M. H. Characterization of Sputter-Coated Polyethylene Naphthalate-Foil as Novel Flexible Surface DBD Plasma Source. *Plasma Medicine* **13** (2023).
45. Alfvén, H. The plasma universe. *Physics Today* **39,** 22–27 (1986).
46. Lu, X. *et al.* An *RC* plasma device for sterilization of root canal of teeth. *IEEE transactions on Plasma Science* **37,** 668–673 (2009).
47. Kazemi, A., Nicol, M. J., Bilén, S. G., Kirimanjeswara, G. S. & Knecht, S. D. Cold Atmospheric Plasma Medicine: Applications, Challenges, and Opportunities for Predictive Control. *Plasma* **7,** 233–257 (2024).

48. Müller, M. *Characterisation of cold atmospheric plasma afterglow for decontamination* in (2019). https://api.semanticscholar.org/CorpusID:208709389.
49. Stoffels, E., Sakiyama, Y. & Graves, D. B. Cold Atmospheric Plasma: Charged Species and Their Interactions With Cells and Tissues. *IEEE Transactions on Plasma Science* **36,** 1441–1457 (2008).
50. Von Keudell, A. *Einführung in die Plasmaphysik* Vorlesungsskript. https://www.ep2.ruhr-uni-bochum.de/files/skripte/skriptpp.pdf [Accessed: 14.02.2025].
51. Kondeti, V. S. K. *et al.* Long-lived and short-lived reactive species produced by a cold atmospheric pressure plasma jet for the inactivation of Pseudomonas aeruginosa and Staphylococcus aureus. *Free Radical Biology and Medicine* **124,** 275–287. ISSN: 0891-5849. https://www.sciencedirect.com/science/article/pii/S0891584918309304 (2018).
52. Lecointre, G. & Le Guyader, H. *The tree of life: a phylogenetic classification* (Harvard University Press, 2006).
53. Page, R. D. & Holmes, E. C. *Molecular evolution: a phylogenetic approach* (John Wiley & Sons, 2009).
54. Woese, C. R., Kandler, O. & Wheelis, M. L. Towards a natural system of organisms: proposal for the domains Archaea, Bacteria, and Eucarya. *Proceedings of the National Academy of Sciences* **87,** 4576–4579 (1990).
55. Beveridge, T. J. Use of the Gram stain in microbiology. *Biotechnic & Histochemistry* **76,** 111–118 (2001).
56. Tripathi, N. & Sapra, A. Gram staining (2020).
57. Mattern, R. *File:Zellwand-Gramfärbung Grau.svg* https://commons.wikimedia.org/w/index.php?curid=10474005 [Accessed: 14.02.2025]. 2010.
58. Mai-Prochnow, A., Clauson, M., Hong, J. & Murphy, A. B. Gram positive and Gram negative bacteria differ in their sensitivity to cold plasma. *Scientific reports* **6,** 38610 (2016).
59. Laroussi, M., Mendis, D. & Rosenberg, M. Plasma interaction with microbes. *New Journal of Physics* **5,** 41 (2003).
60. Santos, A. L. S. d. *et al.* What are the advantages of living in a community? A microbial biofilm perspective! *Memórias do Instituto Oswaldo Cruz* **113,** e180212 (2018).
61. Knaysi, G. The endospore of bacteria. *Bacteriological reviews* **12,** 19–77 (1948).
62. Pina-Perez, M. C., Martinet, D., Palacios-Gorba, C, Ellert, C. & Beyrer, M. Low-energy short-term cold atmospheric plasma: controlling the inactivation efficacy of bacterial spores in powders. *Food Research International* **130,** 108921 (2020).
63. Van Bokhorst-van de Veen, H. *et al.* Inactivation of chemical and heat-resistant spores of Bacillus and Geobacillus by nitrogen cold atmospheric plasma evokes distinct changes in morphology and integrity of spores. *Food microbiology* **45,** 26–33 (2015).
64. Deng, X., Shi, J. & Kong, M. G. Physical mechanisms of inactivation of Bacillus subtilis spores using cold atmospheric plasmas. *IEEE Transactions on Plasma Science* **34,** 1310–1316 (2006).

65. Tschang, C.-Y. T. & Thoma, M. Biofilm inactivation by synergistic treatment of atmospheric pressure plasma and chelating agents. *Clinical Plasma Medicine* **15,** 100091 (2019).

66. Gilmore, B. F. *et al.* Cold plasmas for biofilm control: opportunities and challenges. *Trends in biotechnology* **36,** 627–638 (2018).

67. Schütte, T. *Was bedeuten Log-Stufen?* `https://desitek.de/was-bedeuten-log-stufen/` [Accessed: 14.02.2025].

68. UVSmart. *Was ist die Protokollreduzierung und wofür wird sie verwendet?* `https://de.uvsmart.nl/articles/what-is-log-reduction-and-what-is-it-used-for` [Accessed: 14.02.2025]. 2022.

69. Sella, S. R., Vandenberghe, L. P. & Soccol, C. R. Bacillus atrophaeus: main characteristics and biotechnological applications–a review. *Critical reviews in biotechnology* **35,** 533–545 (2015).

70. Of Microorganisms, L. I. D.-G. C. & GmbH, C. C. *Catalogue* `https://www.dsmz.de/collection/catalogue/details/culture/DSM-30923` [Accessed: 27.03.2025]. 2010.

71. GmbH, S. *Simicon Qualitätszertifikat Sporensuspension* 2019.

72. Paik, W., Sherry, E. & Stern, J. Thermal death of Bacillus subtilis var. niger spores on selected lander capsule surfaces. *Applied Microbiology* **18,** 901–905 (1969).

73. Blount, Z. D. The unexhausted potential of E. coli. *elife* **4,** e05826 (2015).

74. Chiappim, W. *et al.* Antimicrobial effect of plasma-activated tap water on Staphylococcus aureus, Escherichia coli, and Candida albicans. *Water* **13,** 1480 (2021).

75. Hantke, K. Compilation of Escherichia coli K-12 outer membrane phage receptors–their function and some historical remarks. *FEMS Microbiology Letters* **367,** fnaa013 (2020).

76. Niveditha, A *et al.* Application of cold plasma and ozone technology for decontamination of Escherichia coli in foods-a review. *Food control* **130,** 108338 (2021).

77. Wang, Q. & Salvi, D. Evaluation of plasma-activated water (PAW) as a novel disinfectant: Effectiveness on Escherichia coli and Listeria innocua, physicochemical properties, and storage stability. *Lwt* **149,** 111847 (2021).

78. Becker, M, Gies, M, Polity, A, Chatterjee, S & Klar, P. Materials processing using radio-frequency ion-sources: Ion-beam sputter-deposition and surface treatment. *Review of scientific instruments* **90** (2019).

79. SynFlex Elektro GmbH [Internet]. *Data Sheet Teonex® Q5100 PEN foil* Available from: `https://www.synflex.com/insulate/syntherm-isolierstoffe/detail/teonexr-q5100-6/`. c2020 [Cited 2023 Jul 13].

80. Liren Electrical Insulation Materials [Internet]. *Product Show Teonex PEN Film* Available from: `http://www.liren01.com/ProductShow.asp?ArticleID=246`. c2013 [Cited 2022 Nov 22].

81. Staicopolus, D. The computation of surface tension and of contact angle by the sessile-drop method. *Journal of Colloid Science* **17,** 439–447 (1962).

82. Owens, D. K. & Wendt, R. Estimation of the surface free energy of polymers. *Journal of applied polymer science* **13,** 1741–1747 (1969).

83. Rabel, W. Einige Aspekte der Benetzungstheorie und ihre Anwendung auf die Untersuchung und Veränderung der Oberflächeneigenschaften von Polymeren. *Farbe und Lack* **77,** 997–1005 (1971).
84. Kaelble, D. Dispersion-polar surface tension properties of organic solids. *The Journal of Adhesion* **2,** 66–81 (1970).
85. Ström, G., Fredriksson, M. & Stenius, P. Contact angles, work of adhesion, and interfacial tensions at a dissolving hydrocarbon surface. *Journal of colloid and interface science* **119,** 352–361 (1987).
86. Ohm, A & Lippold, B. Charakterisierung der Benetzbarkeit von Arzneistoffpulvern mit Hilfe der Sessile Drop-Technik. II: Kritische Oberflächenspannung und Randwinkel/Oberflächenspannungs-Kurven. *Pharmazeutische Industrie* **48,** 508–513 (1986).
87. Nefedov, V. *X-Ray Photoelectron Spectroscopy of Solid Surfaces* ISBN: 9781466564732. `https://books.google.de/books?id=agmmEAAAQBAJ` (CRC Press, 2023).
88. Shimizu, T., Sakiyama, Y., Graves, D. B., Zimmermann, J. L. & Morfill, G. E. The dynamics of ozone generation and mode transition in air surface microdischarge plasma at atmospheric pressure. *New Journal of Physics* **14,** 103028 (2012).
89. Bass, A. & Paur, R. *The ultraviolet cross-sections of ozone: I. The measurements* in *Atmospheric Ozone: Proceedings of the Quadrennial Ozone Symposium held in Halkidiki, Greece 3–7 September 1984* (1985), 606–610.
90. Hołub, M. On the measurement of plasma power in atmospheric pressure DBD plasma reactors. *International Journal of Applied Electromagnetics and Mechanics* **39,** 81–87 (2012).
91. Fatima, H. *et al.* Spectroscopic evaluation of vibrational temperature and electron density in reduced pressure radio frequency nitrogen plasma. *SN Applied Sciences* **3,** 1–11 (2021).
92. Selivonin, I, Lazukin, A, Moralev, I, Krivov, S & Roslyakov, I. *Erosion of the sputtered electrodes in the surface barrier discharge* in *Journal of Physics: Conference Series* **1394** (2019), 012027.
93. Houser, N. *et al.* Microfabrication of dielectric barrier discharge plasma actuators for flow control. *Sensors and Actuators A: Physical* **201,** 101–104 (2013).
94. Eto, H., Ono, Y., Ogino, A. & Nagatsu, M. Low-temperature sterilization of wrapped materials using flexible sheet-type dielectric barrier discharge. *Applied physics letters* **93** (2008).
95. Gershman, S. *et al.* A low power flexible dielectric barrier discharge disinfects surfaces and improves the action of hydrogen peroxide. *Scientific reports* **11,** 4626 (2021).
96. Lee, S., Jung, S. & Kim, D.-G. Surface dielectric barrier discharge devices for low voltage and low power radical sheet. *Clinical Plasma Medicine* **9,** 5 (2018).
97. Boekema, B. *et al.* A new flexible DBD device for treating infected wounds: in vitro and ex vivo evaluation and comparison with a RF argon plasma jet. *Journal of Physics D: Applied Physics* **49,** 044001 (2015).
98. Gail, J., Schmidt, A. & Thoma, M. H. A Novel Approach on Dielectric Barrier Discharge Using Printed Circuit Boards. *IEEE Transactions on Radiation and Plasma Medical Sciences* **7,** 307–313 (2022).

99. Nagai, M. & Takakuda, K. Influence of number of dental autoclave treatment cycles on rotational performance of commercially available air-turbine handpieces. *Journal of medical and dental sciences* **53,** 93–101 (2006).

100. Worthington, L & Martin, M. An investigation of the effect of repeated autoclaving on the speed of some dental turbines in general dental practice. *Journal of dentistry* **26,** 75–77 (1998).

101. Baier, R. *et al.* Degradative effects of conventional steam sterilization on biomaterial surfaces. *Biomaterials* **3,** 241–245. ISSN: 0142-9612. https://www.sciencedirect.com/science/article/pii/0142961282900278 (1982).

102. Han, A., Tsoi, J. K., Matinlinna, J. P., Zhang, Y. & Chen, Z. Effects of different sterilization methods on surface characteristics and biofilm formation on zirconia in vitro. *Dental Materials* **34,** 272–281. ISSN: 0109-5641. https://www.sciencedirect.com/science/article/pii/S0109564117304360 (2018).